Egyptian Journal of Soil Science

http://ejss.journals.ekb.eg/

Effect of Chitosan/jojoba oil/ZnO nanocomposite Capsules Applications on Some Chemical Properties of Polluted Soils

Doaa T. Eissa

Soil Physics and Chemistry dept., Water resources and desert land division, Desert Research Center, Cairo, P.O.B 11753, Egypt

USING chitosan/jojoba oil and chitosan/jojoba oil/ZnO nanocomposite capsules, this study looked at how to get rid of Fe^{2+} and Ni^{2+} ions from soil in study areas with high levels of heavy metals like Fe^{2+} and Ni^{2+} ions, which pose environmental risks to the ecosystem. The created adsorbents were characterized using scanning electron microscopy (SEM), Fourier transform infrared (FTIR), particle size measurements and transmission electron microscopy (TEM). A batch experiment was performed to determine the effects of contact time, adsorbate concentration, temperature, and solution pH. At pH 3.3 and 5.3, composite materials demonstrated adsorption efficiencies of 90% for Fe^{2+} ions and 69.8% for Ni^{2+} ions from aqueous solutions. According to adsorption isotherm investigations, polymer nanocomposites satisfy the Langmuir and Freundlich models. But the Freundlich isotherm model more accurately characterized the experimental data. The study results suggested that chitosan/jojoba oil and chitosan/jojoba oil/ZnO nanocomposite capsules serve as practical materials for removing Fe^{2+} and Ni^{2+} ions from aqueous solutions. These capsules can be utilized as fertilizers, especially in soils contaminated with Fe and Ni, while providing Mallow plant (*Corchorus olitorius*) nutrients like Zn.

Key words: Green Polymer; Polluted Soil; Heavy Metals; Nanomaterials.

1. Introduction

Heavy metals accumulate in living organisms through absorption and storage processes rather than being effectively removed (Nnaji et al., 2023). Heavy metal pollution harms drinking water, the food chain, and soil. Contamination by metal ions such as Fe (II), Ni (II), Pb (II), Cd (II), and Cu (II) can be attributed to various human activities. These activities encompass manufacturing, mining, smelting, fertilizer and pesticide usage, traffic emissions, municipal waste disposal, industrial effluents, and the release of industrial chemicals, all of which have been increased in recent years (Alengebawy et al., 2021). The presence of hazardous ions in bodies of water negatively influences water quality (Akhtar et al., 2021). The agricultural sector is confronted with multiple challenges, including lower crop yields, different difficulties, such as environmental contamination and nutrient insufficiency (Zain et al., 2023). Heavy metal contamination in the environment is a significant issue in several countries. Over the last two decades, considerable attempts have been made to minimize pollution sources and remediate damaged soil and water resources (Xu et al., 2020). Adsorption is a low-cost method for removing inorganic contaminants from water. Nevertheless, it is essential to consider the primary disadvantages of the adsorption process, including the costs associated with regeneration, the selection of an appropriate adsorbent for treating specific wastewater discharges, and the nature of contaminants present in this wastewater (Maftouh et al., 2023).

There has been a recent surge in interest in developing "green polymers" derived from natural resources (Ghadhban et al., 2023). Polymer blending is one of the most efficient approaches for developing novel materials with desired qualities. Although biopolymers demonstrated their promise, it is critical to enhance several of their features to the

*Corresponding author e-mail: doaataha1378@gmail.com
Received: 02/02/2024; Accepted: 22/02/2024
DOI: 10.21608/EJSS.2024.267370.1716

point where they can compete with petroleum derivatives, particularly addressing issues related to their poor mechanical, barrier, processing, and thermal capabilities. Chitosan, known as poly (1-4)-d-glucosamine, is a deacetylated chitin, a non-toxic substance that can be produced in huge quantities from shrimp and crab shells. One of chitosan's most valuable qualities is its ability to selectively bind desirable elements, such as metal ions (Marturano et al., 2023). Due to its high nitrogen content, chitosan is an influential electron donor, making it a potent chelating agent with a high adsorption capacity for hazardous metal ions such as copper, lead, mercury, and uranium in wastewater. Many studies have shown that crosslinking, regulated N-acylation, and N-alkylation with various functional groups can increase chitosan's chelating activity. Chitosan (the only pseudo-natural polycationic chemical) and its electrostatic complexes made from natural or synthetic polymers are used to enclose fertilizer for controlled release and encapsulation.

Chitosan-based products offer advantages such as biodegradability, hydrophilic properties, and the presence of polar groups capable of secondary interactions with other polymers. These interactions include hydrogen bonding through -OH and -NH_2 groups and hydrophobic interactions involving N-acetyl groups (Ali et al., 2022). Chitosan is another renewable biopolymer that has been widely employed in the production of natural hydrogels. However, chitosan-based hydrogels often lack mechanical stability unless crosslinked or strengthened with appropriate chemicals. In 2006, the global output of caught and farmed shrimp surpassed 6 million tons reported by FAO in 2009. Only 60% is used for food, leaving 2.3 million tons for non-food purposes. Shrimp waste, which contains chitin, proteins, lipids, pigments, and taste components, has economic significance in the food sector (Khandegar et al., 2021). Recently, using nutritional components in agriculture in the form of nanoparticles (NPs) has been recognized as an effective strategy to increase crop development. The element nanoforms may minimize nutrient losses and promote crop development (Farooq et al., 2022; Faizan et al., 2023 and Mahmoud et al., 2023). Among metal-based NPs, there is growing interest in using zinc oxide (ZnO) NPs as a fertilizer in agriculture (Hyder et al., 2023). Besides, chitosan is a valuable soil amendment. As a result, in this work, we created a chitosan composite by integrating nano-zinc oxide (nano-ZnO) to enhance chitosan's chemical characteristics (Zungu et al., 2023). Because of their amazing unique and chemical characteristics, zinc oxide (ZnO) nanoparticles are the most promising nano-agents. Human cells are not harmed by nano-ZnO. The Food and Drug Administration (FDA) of the United States has approved nano-ZnO as a safe substance (Rahman et al., 2022). The fast biological synthesizing of zinc nanoparticles with jojoba oil is an environmentally safe, easy, and efficient technique for nanoparticle synthesis. Using jojoba oil eliminates the need for hazardous and toxic reducing and stabilizing agents found in other chemical components (Ashour et al., 2023 and Sári et al., 2024a). Jojoba oil consists of 60% wax esters, composed of fatty acids and alcohols with chain lengths ranging from C20 to C26 (Wenning et al., 2019).

Sodium lauryl sulfate (SLS) is an anionic surfactant derived from coconut and/or palm kernel oil, primarily composed of sodium alkyl sulfates, particularly lauryl. It serves as a surfactant, reducing the surface tension of aqueous solutions (Nirmala et al., 2021). Chitosan/jojoba oil/ZnO nanocomposite capsules exhibit a larger surface area-to-volume ratio with reduced particle size, dispersion, and altered shape. The stability of these nanoparticles is influenced by environmental conditions, leading to the development of agglomerates (Wojcieszek et al., 2023). To address the demand for environmentally friendly nanoparticles, researchers are exploring green technologies to produce various metal nanoparticles for agricultural applications. This approach is driven by the toxicity and non-eco-friendly by-products associated with the chemicals used in traditional nanoparticle manufacturing and stabilization processes.

Biological methods for synthesizing metal nanoparticles utilizing plant extracts, such as jojoba oil, have been proposed as viable alternatives to chemical methods (Kurhade et al., 2021 and Hamdy et al., 2023).

The mallow plant (*Corchorus olitorius*) is noteworthy for its high iron, potassium, vitamin A, vitamin B6, and vitamin C content. This vegetable holds particular significance in regions where individuals predominantly obtain their energy from micronutrient-deficient staple crops. It is used in folk medicine to treat aches and pains, pectoral pains, enteritis, fever, and tumours. In addition, the leaves are used to treat cystitis, fever, dysuria, and gonorrhoea. It possesses anti-inflammatory activities and gastro-protective qualities (Ahmed and Sarkar, 2022). The present work aimed to investigate the effect of chitosan/jojoba oil and the chitosan/jojoba

oil/ZnO nanocomposite capsules as soil ameliorants to improve agricultural productivity of polluted soils, especially those contaminated with Fe and Ni. Furthermore, the study aimed to address the management of agricultural waste, specifically chitosan, focusing on recycling possibilities. Finally, the study investigated the efficacy of chitosan/jojoba oil and chitosan/jojoba oil/ZnO nanocomposite capsules in removing Fe^{2+} and Ni^{2+} from solutions.

2. Material and Methods

2.1. Soil sampling and analysis

The soil contaminated with anthropogenic sources was collected from EL-Gabal EL- Asfer (30° 13′ 27.79″ N, 31° 23′ 4.51″ E), Qalyubia Governorate, Egypt, which is one of the major areas of production of crop, vegetables, and fruits in Cairo. Over the past 70 years, soil contamination with Fe and Ni has occurred due to irrigation with agricultural drainage. Additionally, the long-term application of pesticides and fertilizers might contribute to soil pollution with Fe and Ni. The soil samples underwent the removal of gravel and organic waste through air-drying, crushing, and sieving with a 2-mm sieve. The worldwide pipette method was employed to determine the soil texture. Cottenie (1982) examined the other parameters of the soil samples, including organic matter concentration, pH, electrical conductivity, and $CaCO_3$ content. According to Staff (2014), the total concentration of heavy metals was determined using inductively coupled plasma-optical emission spectroscopy (ICP) following digestion with a combination of HNO_3, H_2SO_4, and $HClO_4$. Chemically extractable heavy metals were extracted using a DTPA + ammonium bicarbonate solution and quantified using the Soltanpour (1985) technique. An inductively coupled plasma emission spectrophotometer (ICPseq-7500) was used to assess the heavy metal concentration.

2.2. Preparation and characterization of chitosan/jojoba oil and the chitosan/jojoba oil/ ZnO nanocomposite capsules

2.2.1. Materials

The used materials were chitosan powder (M.Wt = 1526.5 g mol^{-1}, purity ≥ 97.0%), Zn SO_4 (M.Wt = 161.47 g mol^{-1}, purity ≥ 98%), jojoba oil (obtained from the local market in Egypt), ammonium hydroxide solution (NH_4OH, M.Wt = 35.04 g mol^{-1}, purity ≥ 98%, purchased from Merck Chemicals Ltd.), and sodium dodecyl sulfate (SLS, M.Wt = 288.38 g mol^{-1}, purity ≥ 99%).

2.2.2. Synthesis of chitosan/jojoba oil

The chitosan solution was prepared by adding 5 wt.% chitosan grains to a distilled water solution containing 2 wt.% acetic acid. The mixture was heated to 50°C with stirring for 3 hours. The resulting clear chitosan solution was then cooled to an appropriate temperature and 50 ml of jojoba oil was added. Subsequently, the chitosan was rapidly cross-linked with 5 wt.% glutaraldehyde, resulting in the formation of a brown powder after drying for 24 hours at 70°C in a hot air oven.

2.2.3. Chitosan/jojoba oil/ZnO nanocapsules synthesis

First, the $ZnSO_4$ (10 g) was dissolved in 100 ml of distilled water to prepare ZnO nanoparticles. Second, 100 ml of jojoba oil was added to 100 ml of distilled water heated to 50°C with stirring for 4 hours. Subsequently, a ZnO solution was prepared by adding a $ZnSO_4$ solution to the jojoba oil solution, and the mixture was stirred to achieve uniform mixing at 60°C. To prevent the aggregation of ZnONPs, the pH of the solution was adjusted to 6.06 by adding an ammonium hydroxide solution. The white powder was collected by filtration and extensively washed with ethanol and ultrapure water, Equation 1. The ZnO produced was dried for 24 h at 70°C in a hot air oven and burned at 550°C for 3 h, Equation 2.

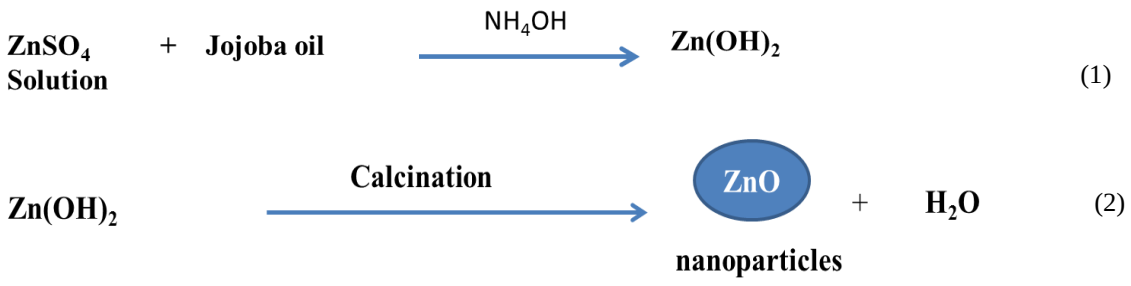

Chitosan solution, prepared as in the previous section, was added to 1g of ZnO nanoparticles in a round flask. Then, 100 ml of jojoba oil was added to 100 ml of distilled water and heated to 50°C with stirring for 4 h using a hand blender. Then, 0.01 g of SLS in 10 ml 2 wt.% acetic acid was added. The reaction mixture was heated at 50°C for 24 h under stirring (500 rpm). After that, chitosan/ZnO nanocapsules were quickly cross-linked with 5 wt.% glutaraldehyde solution. The light brown product was collected by filtration and extensively washed with ethanol and ultrapure water. The sorbent produced was dried for 24 h at 70°C in a hot air oven and then used as adsorbent, as illustrated in Figs. 1 (a , b).

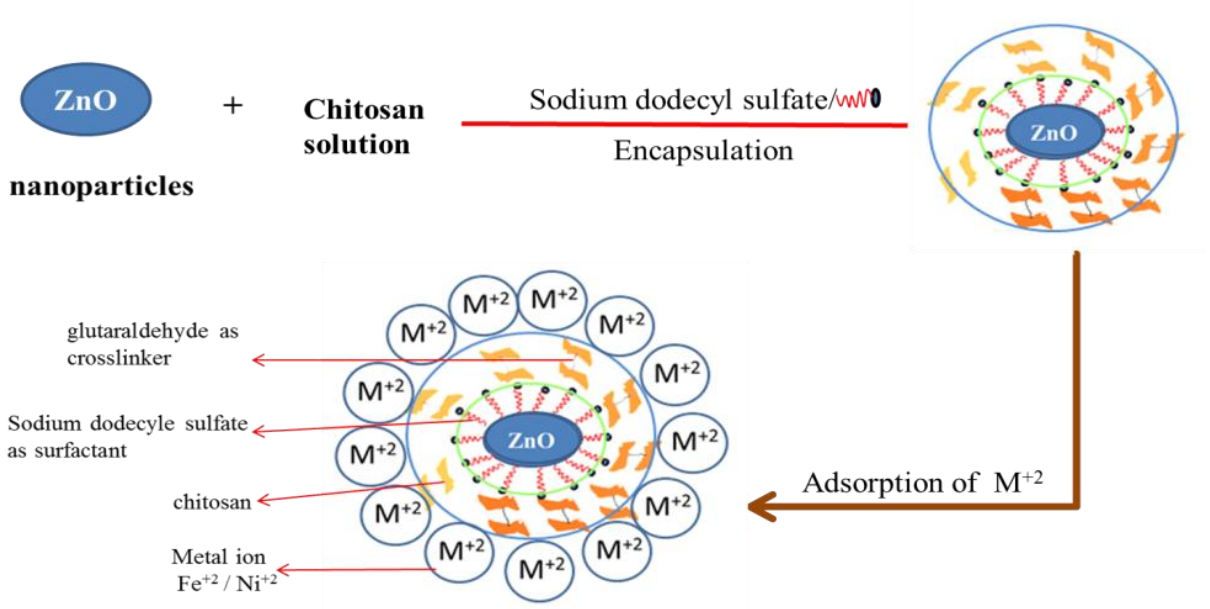

Fig. 1(a). Preparation of chitosan/ jojoba oil /ZnO nanocapsules.

2.2.4. Adsorbent characterization

Fourier transform infrared (FT-IR) spectroscopy was used to identify the particles. A Nicolet Avatar 230 spectrometer assessed the functional groups in the chitosan/jojoba oil and the chitosan/jojoba oil/ZnO nanocomposite capsules adsorbents at room temperature. Scanning electron microscopy (SEM) photographs (Zeiss Auriga) were taken for the two prepared samples. Using dynamic light scattering (DLS, Malvern Zetasizer Nano-ZS Nano Series), the particle size spreading of by chitosan/jojoba oil and the chitosan/jojoba oil/ZnO nanocomposite capsules dispersed in DI water was determined. The size and morphologies of chitosan/jojoba oil and the chitosan/jojoba oil/ZnO nanocomposite capsules were determined by transmission electron microscopy (TEM, JEOL JEM-1010).

2.3. Adsorption process

2.3.1. Effect of concentration

The impact of solution concentration on the removal percentage of Fe^{2+} and Ni^{2+} was investigated. In each 10 ml flask, 0.05 g of chitosan/jojoba oil and chitosan/jojoba oil/ZnO nanocomposite capsules were placed, and 5 ml of solutions with concentrations of 20, 50, 100, and 200 ppm for Fe^{2+} (as $FeSO_4.7H_2O$) and Ni^{2+} (as $NiCl_2$) were added. The mixtures were then equilibrated for 2 hours using a mechanical shaker at 350 rpm and 25°C.

2.3.2. Effect of pH

Experiments were first conducted with chitosan/jojoba oil and the chitosan/jojoba oil/ZnO nanocomposite capsules to determine the optimum pH range where the maximum adsorption of Fe^{2+} and Ni^{2+} was accomplished. The initial pH of the solutions containing Fe^{2+} ranged from about 1.06 to 3.3, while the solutions containing Ni^{2+} had initial pH values ranging from 2.6 to 5.3. The pH levels were meticulously adjusted using dilute HCl and NH_4OH. Subsequently, 5 ml of 50 ppm Fe^{2+} and Ni^{2+} ion solutions, contained in glass bottles and sealed with stoppers, were shaken with 0.05 g of chitosan/jojoba oil and chitosan/jojoba oil/ZnO nanocomposite capsules for 2 hours. The removal percentage of Fe^{2+} and Ni^{2+} was determined at a constant temperature of 298 K.

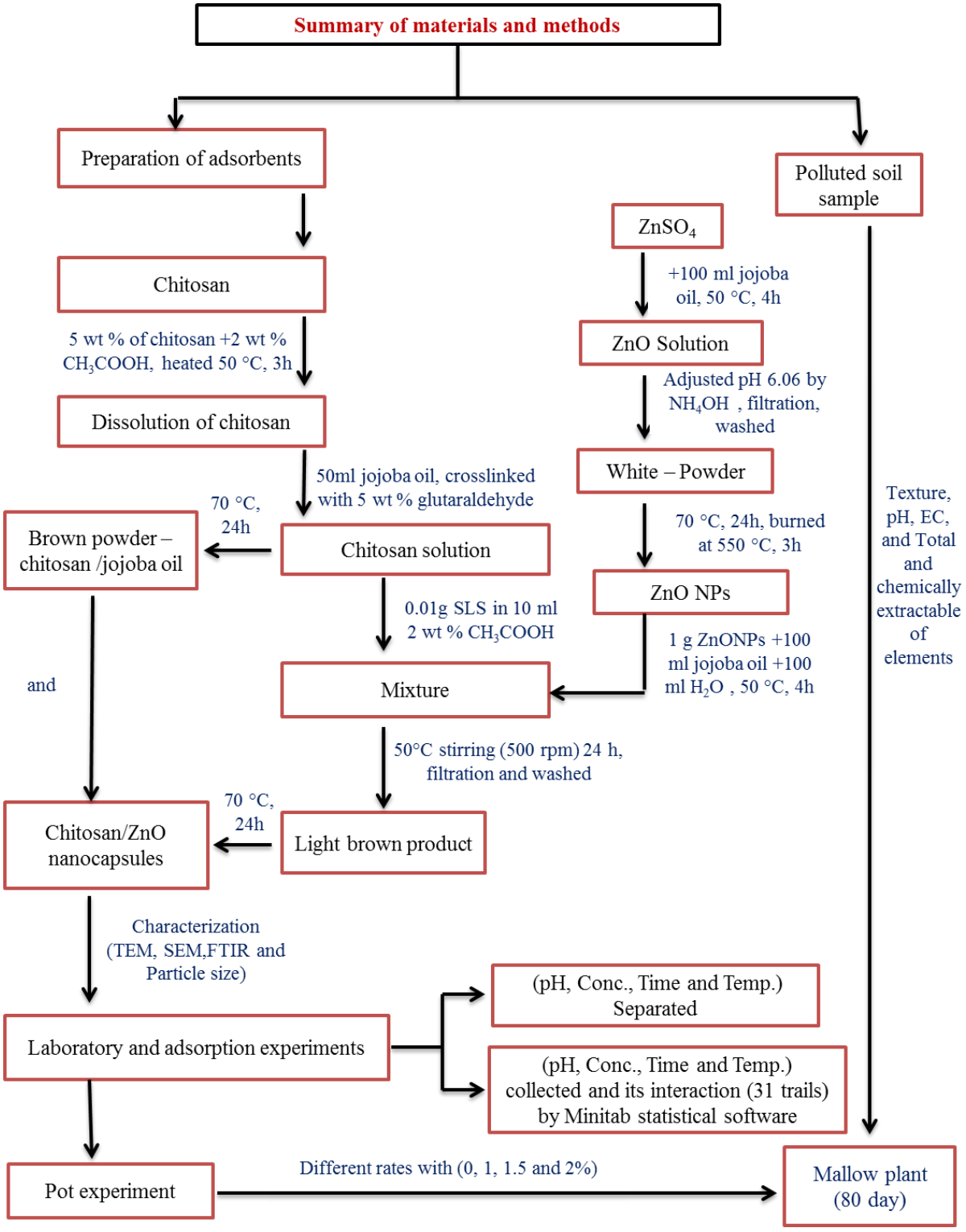

Fig. 1b. Schematic view of preparation and application of chitosan/ZnO nanocomposite nanocapsules and their analyses.

2.3.3. Effect of contact time

The effect of equilibration time on Fe^{2+} and Ni^{2+} removal percentages was investigated. 0.05 g of the chitosan/jojoba oil and the chitosan/jojoba oil/ZnO nanocomposite capsules were contacted for different times ranging from 5 minutes to 6 h with 5 ml of 50

ppm for Fe^{2+} and Ni^{2+} at 298 K, then removal percentage was calculated.

2.3.4 Effect of temperature

The effect of 298, 318, and 338 K on Fe^{2+} and Ni^{2+} adsorptions was investigated under constant experimental conditions. Thus, 0.05 g of chitosan/jojoba oil and the chitosan/jojoba oil/ZnO nanocomposite capsules were contacted with 5 ml of 50 ppm for a shaking time of 2 h, and the removal percentage was then calculated.

2.4 Pot experiment

A pot experiment was conducted to investigate the effect of different soil amendments, of the chitosan/jojoba oil and the chitosan/jojoba oil/ZnO nanocomposite capsules, on the growth and yield of mallow plants grown in polluted soil. Chitosan/jojoba oil and the chitosan/jojoba oil/ZnO nanocomposite capsules amendments were applied at different rates of 0, 1.0, 1.5, and 2.0% w/w of the soil. Soil samples (8 kg) of untreated soil and soil treated with the different amendments were placed in pots in 3 replicates for each treatment. Three mallow plant growth seeds were planted in the pots and then thinned into 2 plants after germination. After 80 days of planting during tap water irrigation, mallow plant shoots were cut at the soil surface and washed with DI water. Shoots were then oven-dried at 70°C for 48 h, weighed for dry matter yield, and ground. At the end of the experiment, soil samples from pots were air-dried and crushed to pass through a 2 mm sieve. After that, pH and EC were determined, and then heavy metals were determined by ICP inductively coupled argon plasma (ICAP).

2.5 Statistical analyses

Using Statistix version 10 (Analytical software, 2018), data from the pot experiment were statistically analyzed, and differences between treatment means were considered significant when they were greater than the least significant difference (L.S.D) at the 5% level.

2.5.1. Design of laboratory experiments:

A response surface methodology (RSM) was used to determine the maximum removal percentage of Fe^{2+} and Ni^{2+}. The central composite design (CCD) method was utilized to obtain the maximum information about the process from the minimum feasible tests. The multivariate research identifies variable interactions and comprehensively examines the experimentally examined topic. This work used a central composite face-centred (CCF) experimental design was used to discover the ideal applications with three levels (1, 0, and +1) for each component. pH (A), concentration (ppm) (B), time (h) (C), and temperature (K) (D) are the operational parameters studied. For Fe^{2+}, the pH, concentration (ppm), time (h), and temperature (K) were set to 3.3-1.06, 20-200 ppm, 5 minutes- 6 hours, and 298-338 K, respectively. For Ni^{2+}, the pH was set at 5.3-2.6. Table 1 displays the coded levels as well as the natural values of the components. Table 2 represents a total of 31 different combinations for removing Fe^{2+} and Ni^{2+} independently from each other. Minitab 16 (Minitab® Statistical Software, 2023) was used to create the experimental design and process the experimental outcomes.

Table 1. Actual and coded values for 4 factors for Fe^{2+} removal.

Parameters	Symbol	Coded factor level		
		-1	0	1
pH	**A**	1.06	2.18	3.30
Conc. (ppm)	**B**	20	110	200
Time (h)	**C**	0.083	3.04	6
Temp. (K)	**D**	298	318	338

Table 2. Central composite design.

Trial	coded variables				decoded variables			
	A	B	C	D	pH	Conc. (ppm)	Time (h)	Temp. (K)
1	-1	-1	-1	-1	1.06	20	0.083	298
2	1	-1	-1	-1	3.3	20	0.083	298
3	-1	1	-1	-1	1.06	200	0.083	298
4	1	1	-1	-1	3.3	200	0.083	298
5	-1	-1	1	-1	1.06	20	6.0	298
6	1	-1	1	-1	3.3	20	6.0	298
7	-1	1	1	-1	1.06	200	6.0	298
8	1	1	1	-1	3.3	200	6.0	298
9	-1	-1	-1	1	1.06	20	0.083	338
10	1	-1	-1	1	3.3	20	0.083	338
11	-1	1	-1	1	1.06	200	0.083	338
12	1	1	-1	1	3.3	200	0.083	338
13	-1	-1	1	1	1.06	20	6.0	338
14	1	-1	1	1	3.3	20	6.0	338
15	-1	1	1	1	1.06	200	6.0	338
16	1	1	1	1	3.3	200	6.0	338
17	-1	0	0	0	1.06	110	3.0415	318
18	1	0	0	0	3.3	110	3.0415	318

Table 2 Cont..

Trial	coded variables			decoded variables				
	A	B		A	B		A	B
19	0	-1	0	0	2.18	20	3.0415	318
20	0	1	0	0	2.18	200	3.0415	318
21	0	0	-1	0	2.18	110	0.083	318
22	0	0	1	0	2.18	110	6.0	318
23	0	0	0	-1	2.18	110	3.0415	298
24	0	0	0	1	2.18	110	3.0415	338
25	0	0	0	0	2.18	110	3.0415	318
26	0	0	0	0	2.18	110	3.0415	318
27	0	0	0	0	2.18	110	3.0415	318
28	0	0	0	0	2.18	110	3.0415	318
29	0	0	0	0	2.18	110	3.0415	318
30	0	0	0	0	2.18	110	3.0415	318
31	0	0	0	0	2.18	110	3.0415	318

3. Results

The initial analysis of soil properties (Table 3) revealed that the soil was only polluted with Fe^{2+} and Ni^{2+}, whose levels exceeded the soil's allowed limits. This area's soil is primarily loamy sand (Table 3). Standard procedures were used to establish the physiochemical properties of the soil as well as trace element concentrations. A pH meter measured soil pH at a 1:2.5 soil-to-water ratio.

Table 3. Some physical and chemical properties of the contaminated soils collected from EL- Gabal El-Asfer, Egypt.

Particle size distribution (%)		
Sand	80.3	
Silt	7.90	
Clay	11.8	
Texture class	Loamy sand	
Properties	**Value**	
OM (%)	3.90	
$CaCO_3$ (%)	8.30	
pH (1:2.5)	7.80	
EC (dS m^{-1})	2.75	
Elements (ppm)	**Total**	**Available**
Fe*	10780.3	41.9
Ni*	59.9	7.99
Mn	481	67.5
Zn	243.3	29.5
Cr	104.1	9.65
Pb	118.4	39.3
Co	27.03	0.01

3.1. Characterization

The functional groups involved in the binding mechanism between chitosan and ZnO NPs were identified using FTIR analysis of chitosan/jojoba oil and chitosan/jojoba oil/ZnO nanocomposite capsules. Both chitosan/jojoba oil and chitosan/jojoba oil/ZnO nanocomposite capsules exhibited identical characteristic peaks, with only minor differences observed during chitosan/jojoba capsulation, as shown in Fig. 2.

The morphological structure of (Chitosan/jojoba oil) and (chitosan/jojoba oil/ZnO nanocomposites) are presented in Fig. 3 (a, b).

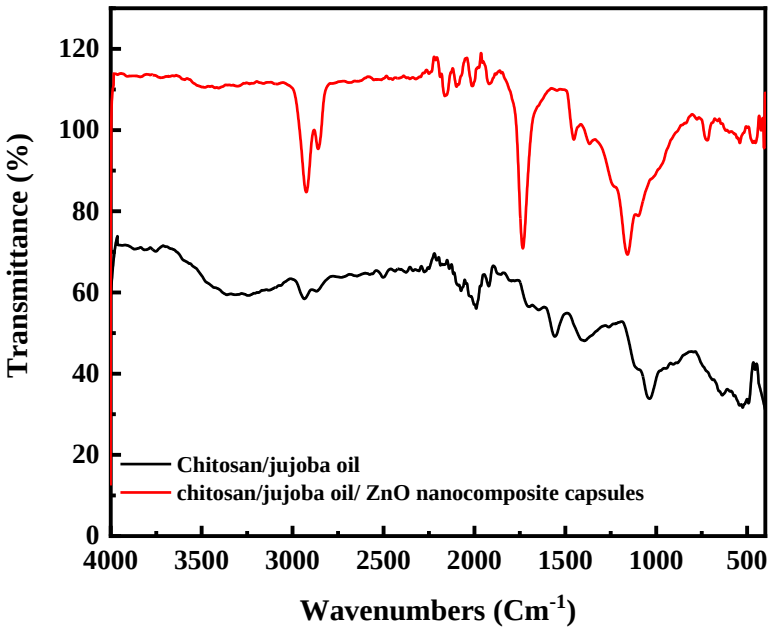

Fig. 2. FTIR spectra of chitosan/jojoba oil and chitosan/jojoba oil/ZnO nanocomposite capsules.

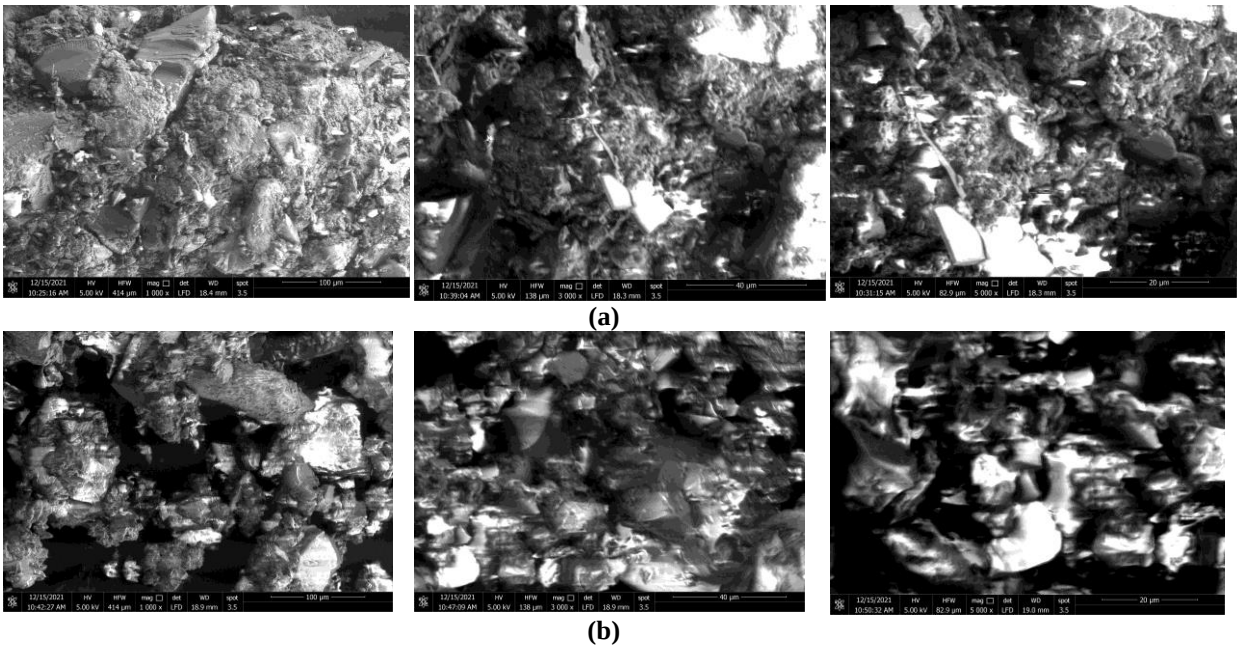

Fig. 3 SEM images of (a) chitosan/jojoba oil and (b) chitosan/jojoba oil/ZnO nanocomposite capsules.

According to the particle size analysis, the mean size of the blank (chitosan/jojoba oil) was approximately 38.3 nm, and the mean size of the capsules (chitosan/jojoba oil/ZnO nanocomposite capsules) was 24.6 nm (Figure 4-1). As a result, the particle size distributions of nanocapsules are sufficient for heavy metal removal.

TEM images gave us information on the particle shape and the determination of particle size. Typical TEM micrograph of chitosan/jojoba oil and chitosan/jojoba oil/ZnO nanocomposite capsules was shown in Figure (4-2).

From TEM images, Fig. (4-2) the aggregation of chitosan/jojoba oil and chitosan/jojoba oil/ZnO nanocomposite capsules with variety of shapes most of them are capsules and a few of which are random shapes and the analysis of chitosan/jojoba oil diameter ranged from 26-29 nm. While the diameter of chitosan/jojoba oil/ZnO nanocomposite capsules ranged between 10-15 nm. ZnO NPs were well-coated by chitosan/jojoba oil which confirmed with DLS results.

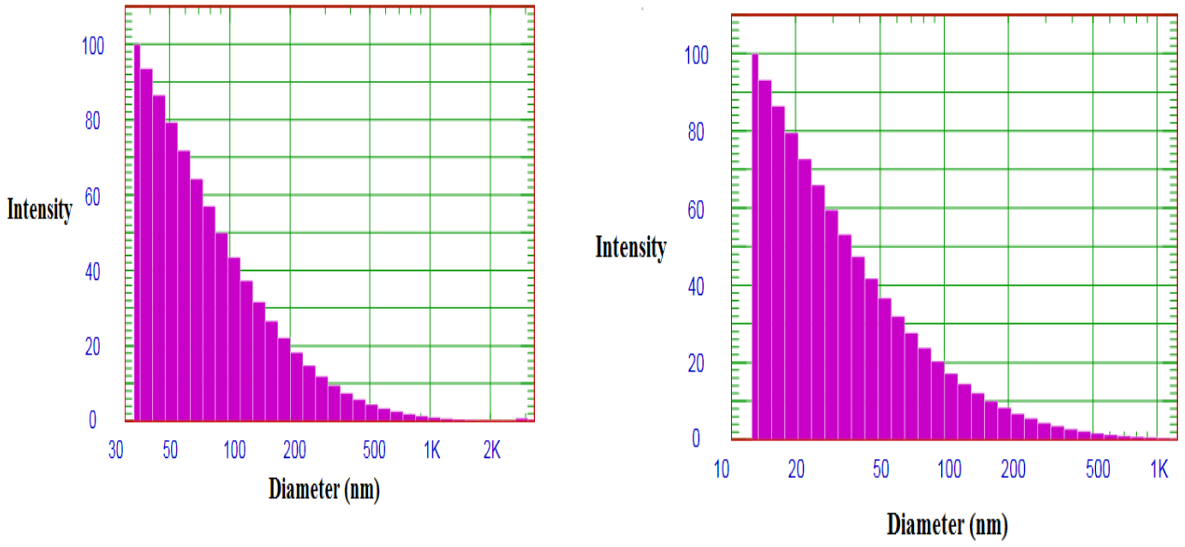

(a)chitosan/jojoba oil **(b) chitosan/jojoba oil/ ZnO nanocomposite capsules**

Fig. 4-1. Particle size distribution of (a) chitosan/jojoba oil and (b) chitosan/jojoba oil/ ZnO nanocomposite capsules.

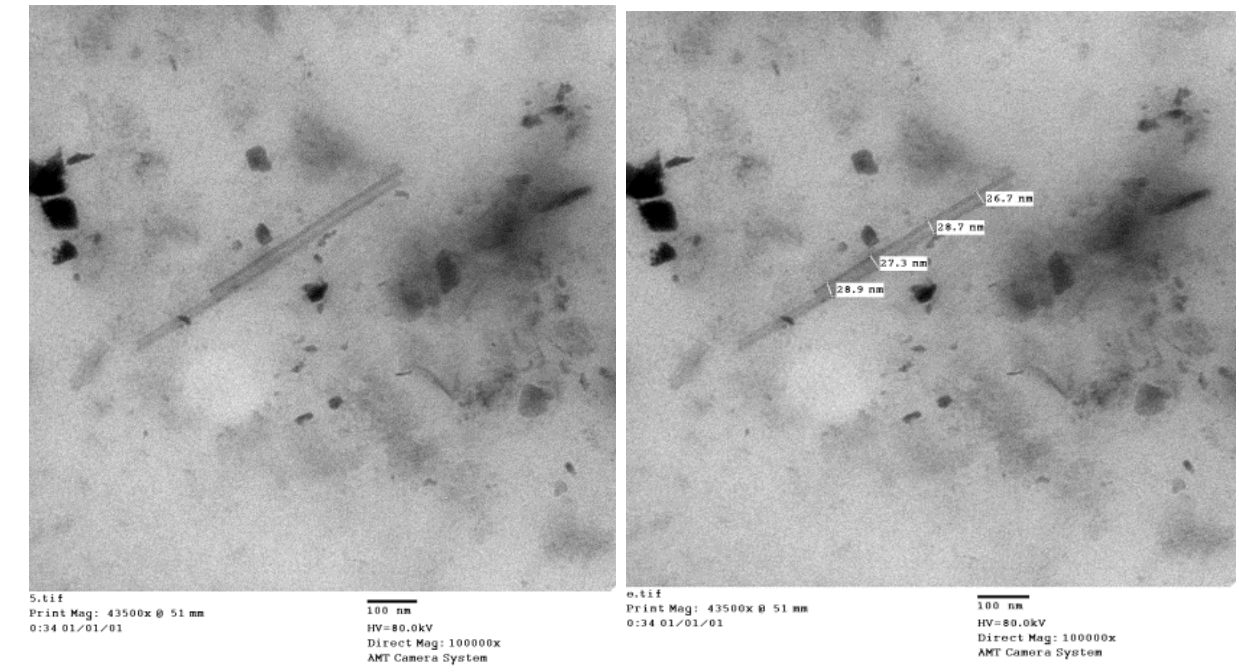

(a)

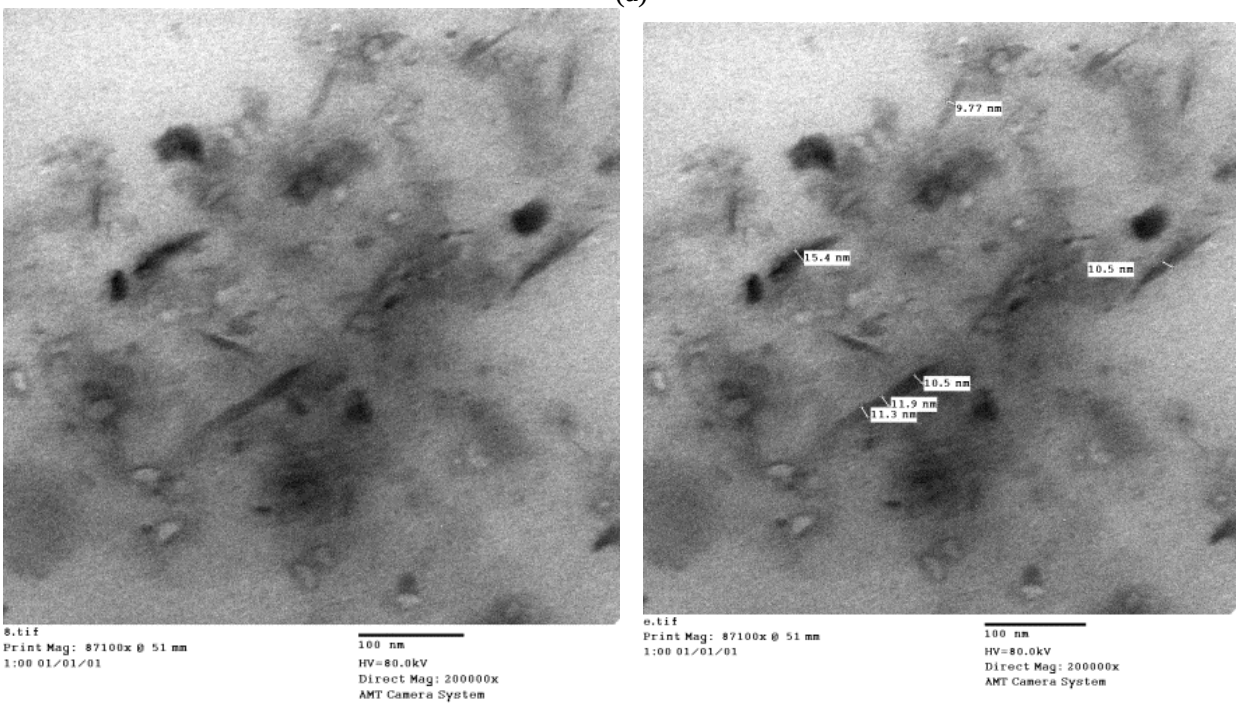

(b)

Fig. 4-2. TEM images of (a) chitosan/jojoba oil and (b) chitosan/jojoba oil/ ZnO nanocomposite capsules.

3.2. Adsorption experiments

3.2.1. Effect of concentration

According to increasing specific surface areas of powders and exchangeable processes, Fe^{2+} and Ni^{2+} removal percentages increased for chitosan/jojoba oil/ZnO nanocomposite capsules > chitosan/jojoba oil because the particle sizes of chitosan/jojoba oil and chitosan/jojoba oil/ZnO nanocomposite capsules are 38.3 and 24.6 nm, respectively.

3.2.1.1. Adsorption isotherms

Using Langmuir and Freundlich isotherms, the distribution of Fe^{2+} and Ni^{2+} ions at equilibrium between the surface of sorbent chitosan/jojoba oil and chitosan/jojoba oil/ZnO nanocomposite capsules was investigated.

The linearized form of the Langmuir equation, which is given as Eq. (3), was used to plot the Langmuir isotherm for the adsorption of Fe^{2+} and Ni^{2+}.

$$q_e = \frac{K_L q_m C_e}{1 + K_L C_e} \quad (3)$$

where q_e is the amount of adsorbate (mg g^{-1}), C_e is the adsorbate concentration at equilibrium in solution after adsorption (mg L^{-1}), K_L is the Langmuir constant related to adsorption energy, and q_m is the maximum adsorption capacity (mg g^{-1}).

According to Langmuir, specific adsorption results in homogenized adsorption energy without interaction between the adsorbates and neighboring sites.

The heterogeneous multilayer adsorption system is explained using Freundlich isotherms, and its linearized equation is provided as Eq. (4):

$$\log q_e = \log K_F + 1/n \log C_e \quad (4)$$

where: q_e is the amount of Fe^{2+} or Ni^{2+} adsorbed at equilibrium (mg g^{-1}), and q_m is the maximum adsorption capacity.

The correlation coefficients for the adsorption capacity determined from the isotherm are shown in Table 4 with the Langmuir adsorption constant (L mg^{-1}), the constant C_e, and the constants K_F and n. Compared to the Langmuir model, the Freundlich model provides a better fit to the data.

Table 4. Estimated isotherm parameters for chitosan/jojoba oil and chitosan/jojoba oil/ZnO nanocomposite capsules adsorption of Fe^{2+} and Ni^{2+} ions on various adsorbents.

adsorbate	adsorbent	Langmuir			Freundlich		
		q_m (mg g^{-1})	K_L	R^2	n	K_F (L mg^{-1})	R^2
Fe^{+2}	chitosan/jojoba oil	9.90	0.029	0.95	1.79	0.60	0.97
	chitosan/jojoba oil/ZnO nanocomposite capsules	21.73	0.047	0.90	1.48	1.30	0.97
Ni^{+2}	chitosan/jojoba oil	10.30	0.009	0.81	1.47	0.60	0.99
	chitosan/jojoba oil/ZnO nanocomposite capsules	12.34	0.027	0.88	1.77	1.30	0.99

3.2.2. Effect of pH of solution

Chitosan/jojoba oil/ZnO nanocomposite capsules (0.05 g) were added to 5 ml of Fe^{2+} solutions with pH values ranging from 1.06 to 3.3 and stirred for 2 hours to evaluate the impact of pH. The Fe^{2+} removal percentage increased from 72 to 90 as the potential surface charges of adsorbents were altered by the presence of H^+ or OH^- ions in solutions. On the other hand, as the pH of the solution increases from 2.6 to 5.3, the removal of Ni^{2+} increases from 60.1% to 69.8%, respectively (Fig. 5).

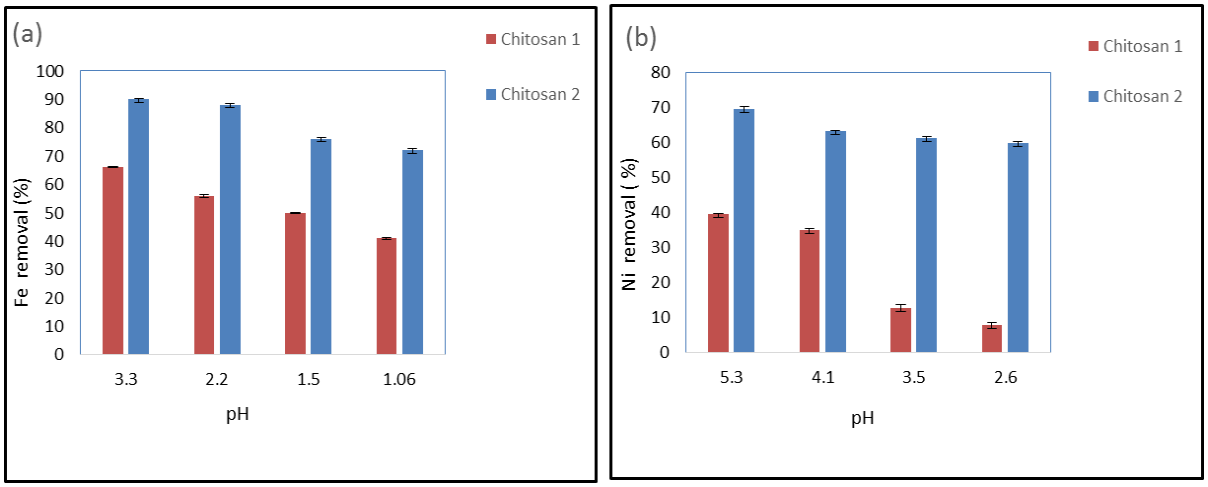

Fig. 5. (a and b) Effects of adsorption pH on removal of Fe^{2+} and Ni^{2+} ion by adsorbents of chitosan 1 (chitosan/jojoba oil) and chitosan 2 (chitosan/jojoba oil/ZnO nanocomposite capsules).

3.2.3. Effect of contact time

The equilibrium time was 1 h for Fe^{2+} and 2 h for Ni^{2+}, while the chitosan/jojoba oil and the chitosan/jojoba oil/ZnO nanocomposite capsules adsorb ions in the order $Fe^{2+} > Ni^{2+}$.

From the obtained data, for all investigated adsorbents, the removal percentage of Fe^{2+} and Ni^{2+}

ions increased with increasing the equilibrium contact time from 5 minutes to 6 h. For chitosan/jojoba oil/ZnO nanocomposite capsules, Fe^{2+} removal increased gradually as reaction time increased from 5 to 30 minutes by about 2%. However, it increased abruptly from 0.5h to 1h by about 9%, constant for 6 h.

The removal percentage of Ni^{2+} ions increased abruptly from 5 minutes to 30 minutes by about 11%, then increased rapidly by about 31% to reach its maximum at 2 hours, after which it remained constant for the next 6 hours.

3.2.4. Effect of temperature

The removal percentage of Fe^{2+} and Ni^{2+} increased with temperature increase. The removal percentage of Fe^{2+} and Ni^{2+} increased gradually from 298 to 318 K by about 2 and 1.2%, respectively. Subsequently, it increased by about 1% for Fe^{2+} and 3% for Ni^{2+} at 338 K.

3.3. Parameters optimization

Chitosan/jojoba oil and chitosan/jojoba oil/ZnO nanocomposite capsules' highest adsorption capability can be determined by conducting trials collected with the parameters optimized simultaneously. The present study used a multivariate design with 31 trials to determine the best parameters' values. The variables or components chosen for the study were the pH, concentration, time, and temperature since they substantially impact the adsorption process. Table 5 lists the expected and experimental results for the sorbents of chitosan/jojoba oil and chitosan/jojoba oil/ZnO nanocomposite capsules and their ability to remove (Fe^{2+} and Ni^{2+} ion), as well as their R^2 and R^2_{adj} values.

Table 5. The expected and experimental results for the sorbents of chitosan/jojoba oil and chitosan/jojoba oil/ZnO nanocomposite capsules.

Trial	chitosan/jojoba oil				chitosan/jojoba oil/ ZnO nanocomposite capsules			
	Fe^{+2}		Ni^{+2}		Fe^{+2}		Ni^{+2}	
	O[1]	P[2]	O	P	O	P	O	P
1	32.9	33.5	5.8	6.0	60.1	57.9	35.8	34.9
2	61.1	60.0	40.2	38.7	76.4	74.9	55.5	54.9
3	27.4	29.1	2.67	3.7	41.3	48.0	25.5	28.6
4	59.1	56.7	36.7	36.6	78.1	72.5	58.7	56.5
5	36.3	40.4	8.9	11.0	64.8	70.6	40.4	44.8
6	67.2	65.9	43.1	42.8	81.5	79.2	61.2	60.5
7	43.7	38.6	10.6	6.9	73.8	61.3	44.4	38.1
8	62.2	65.2	37.4	38.9	70.1	77.4	59.1	61.5
9	36.7	34.4	6.4	4.5	60.9	58.5	37.2	35.7
10	59.1	63.5	32.45	36.6	70.5	78.1	49.4	54.6
11	29.8	30.4	3.9	4.7	50.3	47.8	30.6	30.1
12	63.8	60.5	39.5	37.0	75.7	74.9	60.3	56.8
13	37.1	38.7	11.23	11.8	69.5	70.3	44.9	46.0
14	67.8	66.8	44.3	42.9	83.3	81.5	62.7	60.5
15	35.5	37.3	9.1	10.2	53.8	60.3	38.4	39.9
16	67.7	66.4	41.3	41.6	81.7	79.0	62.4	62.2
17	46.6	43.5	9.1	8.9	63.5	63.3	45.3	44.3
18	68.2	71.3	41.2	41.0	81.4	81.2	63.5	65.4
19	55.9	50.9	15.8	13.9	69.2	65.2	55.4	50.5
20	43.4	48.5	10.5	12.0	55.4	59.0	42.5	48.2
21	48.5	50.2	11.8	11.6	62.4	63.1	49.4	50.3
22	58.3	56.6	16.5	16.3	72.5	71.4	57.9	57.9
23	49.3	49.7	12.34	13.1	64.4	68.7	50.3	51.1
24	51.2	50.8	14.9	13.7	74.5	69.8	51.7	51.8
25	53.3	53.9	13.2	14.0	67.3	67.5	53.2	54.0
26	54.7	53.9	14.7	14.0	68.1	67.5	55.4	54.0
27	54.9	53.9	15.1	14.0	67.3	67.5	56.1	54.0
28	53.9	53.9	13.1	14.0	67.5	67.5	54.9	54.0
29	52.8	53.9	13.5	14.0	66.9	67.5	53.4	54.0
30	54.3	53.9	13.4	14.0	66.3	67.5	54.3	54.0
31	53.2	53.9	13.5	14.0	67.9	67.5	53.1	54.0
R^2 (%)	95.42		98.80		80.46		92.85	
R^2_{adj} (%)	91.41		97.74		63.36		86.60	

1: Observed 2: Predicted

3.4. Analysis of variance (ANOVA)

Table 6, the analysis of variance (ANOVA) was used to assess the model's statistical significance, assessing the variability in the number of components that make up the chitosan/jojoba oil/ZnO nanocomposite capsules adsorption capacity for each effect simultaneously, including interactions and experimental error.

Table 6. Regression equations for the removal of Fe^{2+} and Ni^{2+} ion using different sorbents of chitosan/jojoba oil and chitosan/jojoba oil/ZnO nanocomposite capsules.

Removal % of Fe^{+2} by chitosan/jojoba oil	= 53.86+13.9 pH+3.18 time (h)	(5)
Removal % of Fe^{+2} by chitosan/jojoba oil/ ZnO nanocomposite capsules	=67.51+8.93pH-3.11Conc.(ppm)	(6)
Removal % of Ni^{+2} by chitosan/jojoba oil	=13.96+16.02pH+2.38time (h)+10.99pH^2	(7)
Removal % of Ni^{+2} by chitosan/jojoba oil/ ZnO nanocomposite capsules	=53.97+10.57pH+3.83time(h)+1.94pH*Conc. (ppm)	(8)

The ANOVA results for removing Fe^{2+} and Ni^{2+} ions using adsorbents of chitosan/jojoba oil and chitosan/jojoba oil/ZnO nanocomposite capsules are presented collectively in Table 7. These results demonstrated the effects of large *F* ratios with their corresponding *p*-values less than 0.05, particularly pH, time and concentration. Consequently, the chosen model is appropriate for this research. A mathematical relationship, derived using Minitab statistical software, can be utilized to characterize the quantitative impacts of process variables (pH, concentration, contact time, and temperature) and their interactions on the observed response (removal% of Fe^{2+} and Ni^{2+} ion). After disregarding *p*-values greater than 0.05 in Table 7, mathematical correlations were established connecting the response (removal percentage) with model variables, as defined by the regression equations (5-8).

Table 7. Analysis of variance (ANOVA) for removal % of Fe^{2+} and Ni^{2+} ion by different adsorbent of chitosan/jojoba oil and chitosan/jojoba oil/ZnO nanocomposite capsules.

Source	Chitosan/jojoba oil				Chitosan/jojoba oil/ ZnO nanocomposite capsules			
	Fe^{+2}		Ni^{+2}		Fe^{+2}		Ni^{+2}	
	***F* ratio**	***p* value**	***F* ratio**	***p* value**	***F* ratio**	***P* value**	***F* ratio**	***p* value**
pH	295.72	0.00	1104.86	0.00	43.42	0.00	157.87	0.00
Conc. (ppm)	2.18	0.16	3.62	0.08	5.27	0.04	1.85	0.19
time (h)	15.56	0.00	24.56	0.00	9.53	0.01	20.79	0.00
Temp. (K)	0.43	0.52	0.38	0.55	0.16	0.70	0.20	0.66
pH* pH	2.80	0.11	74.86	0.00	1.75	0.20	0.15	0.70
Conc. (ppm)* Conc. (ppm)	3.87	0.07	0.64	0.44	2.31	0.15	4.27	0.06
time (h)* time (h)	0.04	0.84	0.00	0.99	0.01	0.94	0.00	0.96
Temp. (K)* Temp. (K)	2.84	0.11	0.18	0.67	0.23	0.64	1.30	0.27
pH*Conc.	0.09	0.76	0.01	0.91	1.70	0.21	4.74	0.05
pH*time	0.09	0.77	0.22	0.65	2.11	0.17	1.51	0.24
pH*Temp.	0.53	0.48	0.09	0.76	0.21	0.65	0.11	0.75
Conc. *time	0.57	0.46	0.74	0.40	0.01	0.91	0.02	0.89
Conc. *Temp.	0.01	0.93	1.51	0.24	0.02	0.89	0.03	0.86
time*Temp.	0.55	0.47	1.22	0.29	0.02	0.88	0.01	0.93

3.5. Plots of residuals versus predictions

The plots in Figures 6 (a and b) exhibited a random distribution of residuals along the reference line, with the amplitude of these residuals fluctuating from up to down along the zero line.

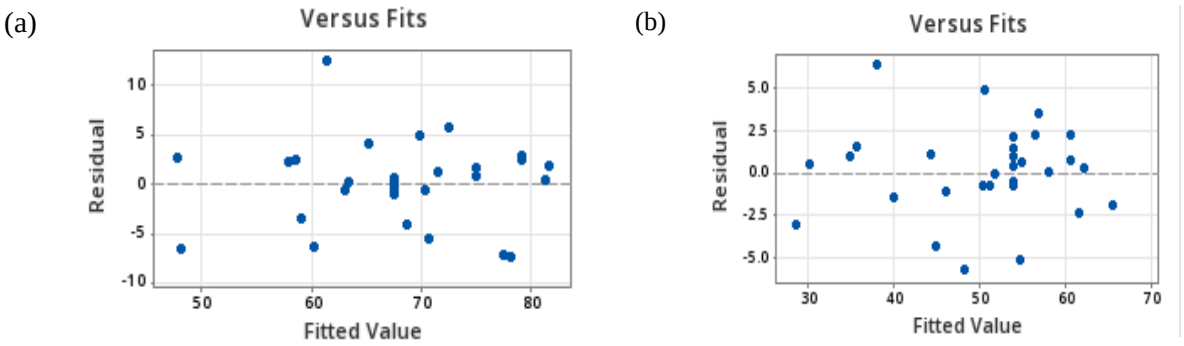

Fig. 6. Random distribution of residuals for removal percentages of (a) Fe^{2+} and (b) Ni^{2+} ions by chitosan/jojoba oil/ZnO nanocomposite capsules.

3.6. Standardized Pareto chart

The Pareto plot revealed that pH (A) and time (D) for Fe removal by chitosan/jojoba oil and pH (A), concentration (B), and time (D) for chitosan/jojoba oil/ZnO nanocomposite capsules exhibited significant impacts. However, temperature (K), pH*pH, concentration (ppm)*concentration (ppm), time (h)*time (h), temperature (K)*temperature (K), pH*concentration, pH*time, pH*temperature, concentration*time, concentration*temperature, and time*temperature did not cross the reference line, indicating their lack of significance in the removal of Fe (Figure 7a).

For the removal of Ni by chitosan/jojoba oil and chitosan/jojoba oil/ZnO nanocomposite capsules, the Pareto plot indicated that pH (A), time (D), and pH^2 (A) for chitosan/jojoba oil, and pH (A), time (D), and pH (A) *concentration (B) for chitosan/jojoba oil/ZnO nanocomposite capsules showed significant impacts, respectively. Other variables did not exhibit significant impacts (Figure 7b).

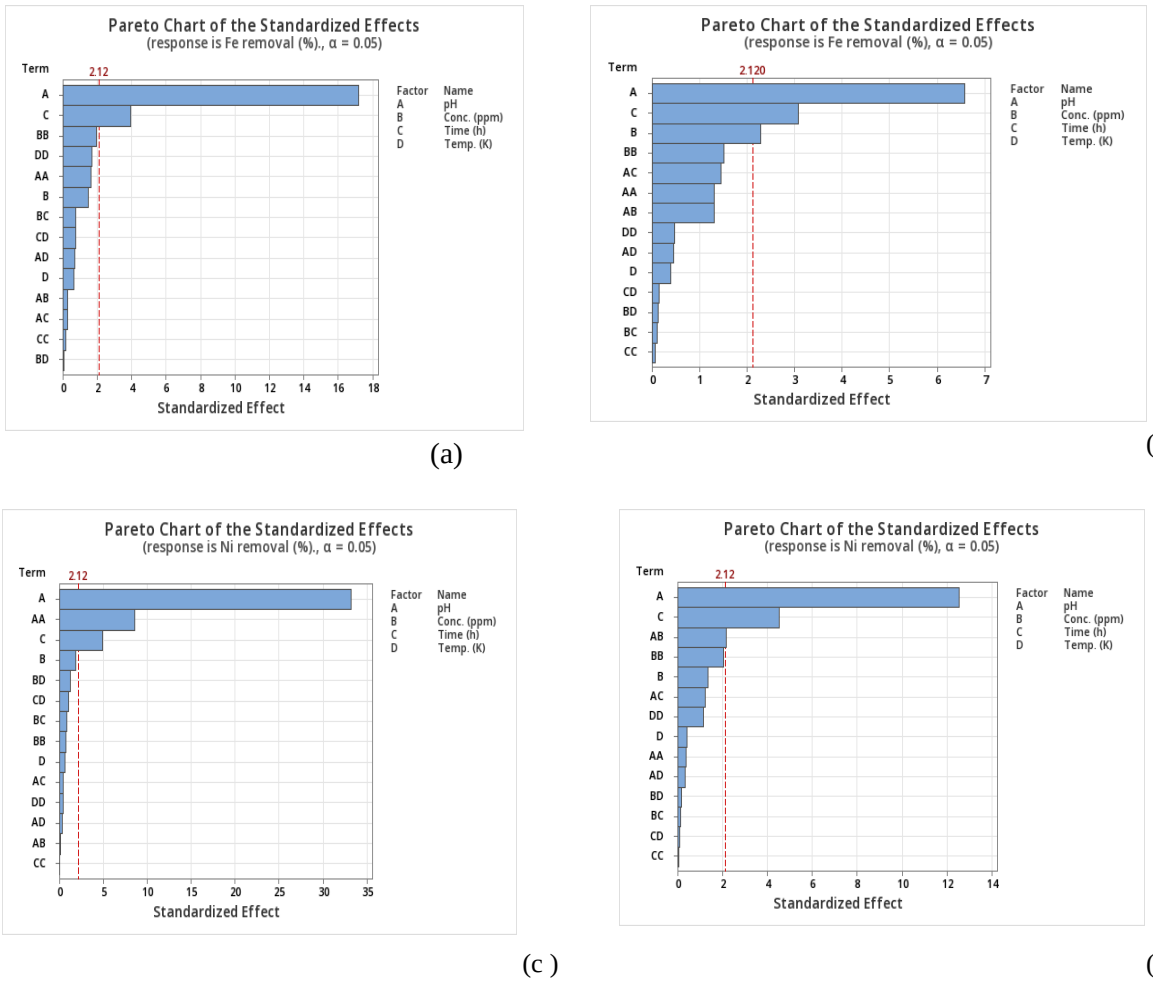

Fig. 7. Standardized Pareto chart for Fe and Ni removal.

3.7. Surface plots and contour plots of response

The predicted response of the variables (removal percentages of Fe^{2+} and Ni^{2+} ion by chitosan/jojoba oil/ZnO nanocomposite capsules) were examined using response surface and contour plots. To examine the interactive effects of parameters (pH, concentration, time, and temperature) on the removal percentage of Fe^{2+} and Ni^{2+} ions by chitosan/jojoba oil/ZnO nanocomposite capsules, refer to Figures 8(a-l) and Figures 9(a-l), respectively.

Figures 8 and 9 (a-f) show graphs illustrating the expected response of Fe^{2+} and Ni^{2+} removal percentages by chitosan/jojoba oil/ZnO nanocomposite capsules adsorbent against any two of the four parameters of pH, concentration, time, and temperature. In comparison, the other two parameters are kept at medium values. Buasri et al. (2024) stated that the surface height impacts the estimated removal percentage. When comparing the various chitosan/jojoba oil and chitosan/jojoba oil/ZnO nanocomposite capsules adsorbents, it was observed that the chitosan/jojoba oil/ZnO nanocomposite capsules had a larger surface area for reactivity.

Generally, the relationship between pH values and the percentage removal of Fe^{2+} and Ni^{2+} ions is favourable at higher initial pH values, as shown in Figures 8 and 9 (a, b, c, d, e, and f). The acidic state increases the competition between Fe^{2+}, Ni^{2+}, and H^{+} for adsorption into the chitosan/jojoba oil/ZnO nanocomposite capsules. Raising the pH reduces competition by increasing the concentration of OH^{-} ions. This demonstrates that the percentage removal of Fe^{2+} and Ni^{2+} ions is better in high pH mediums than in low pH mediums, as more ions are absorbed onto the surface of the as-prepared chitosan/jojoba oil/ZnO nanocomposite capsules. Furthermore, Figures 8 and 9 (c,d,g,h,k, and l) illustrate the relationship between contact duration and removal percentage of Fe^{2+} and Ni^{2+} ions.

These findings indicated that the percentage removal of Fe^{2+} and Ni^{2+} increases with prolonged contact time in the batch adsorption process. Longer contact times enhance the interaction between Fe^{2+} or Ni^{2+} ions and the surfaces of the adsorbent, promoting the adsorption process. Plots a and b in Figure 8 illustrate the reciprocal relationship between pH and concentration; the removal percentage steadily increases as pH increases and Fe^{2+} ion concentration rises. Plots c and d depict the combined impact of pH and shaking duration; the removal percentage rises with both pH and shaking time increases. Moreover, plots e and f illustrate the combined impact of pH and temperature; the removal percentage rises with increased pH. In addition, plots g and h show the interaction between concentration and shaking time; the highest value of Fe removal percentage occurs at 6 hours and a concentration of 55-130 ppm. The interaction between concentration and temperature is depicted in plots i and j; while temperature has a curving relationship with concentration, it decreases as concentration increases. Plots k and l illustrate the impact of shaking duration and temperature; the removal percentage increases rapidly as shaking time increases.

Plots a and b in Figure 9 demonstrate the interaction between pH and concentration; while concentration has a curved relationship with pH, Ni^{2+} removal percentage rapidly increases as pH increases. Plots c and d illustrate the interaction between pH and shaking time; the removal percentage rapidly increases as pH and shaking duration increase. Besides, plots e and f show the combined effect of pH and temperature; the removal percentage rapidly increases with increasing pH while temperature has a curved relationship. Plots g and h demonstrate the interaction between concentration and shaking time; the Ni^{2+} removal percentage progressively rises as shaking time increases, but concentration exhibits a curved relationship. Furthermore, plots i and j show the interactive effect of concentration and temperature; the removal percentage of Ni^{2+} has a curved relationship with both concentration and temperature. Plots k and l show the combined effect of shaking time and temperature; the Ni^{2+} removal percentage increases with increasing the shaking time, while temperature has a curved relationship.

(a)

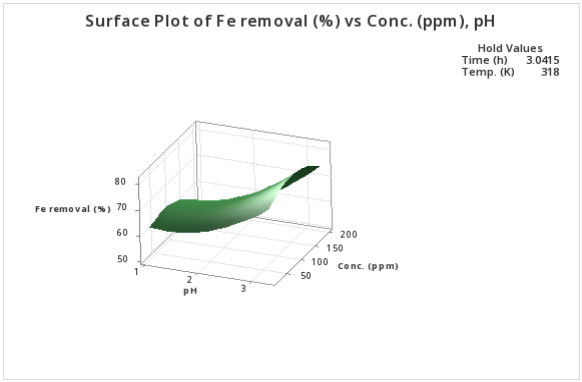
Surface Plot of Fe removal (%) vs Conc. (ppm), pH
Hold Values
Time (h) 3.0415
Temp. (K) 318
Fe removal (%)
80
70
60
50
1
2
3
pH
200
150
100
50
Conc. (ppm)

(b)

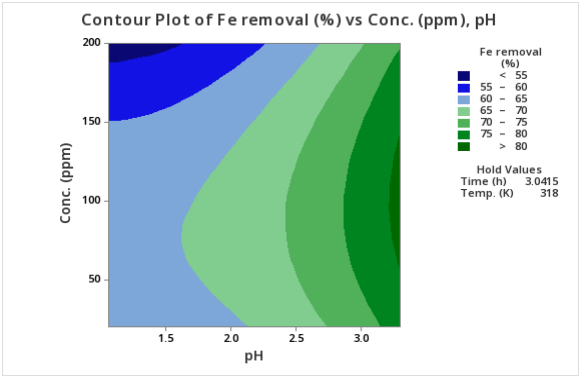
Contour Plot of Fe removal (%) vs Conc. (ppm), pH
Conc. (ppm)
200
150
100
50
1.5
2.0
2.5
3.0
pH
Fe removal (%)
< 55
55 – 60
60 – 65
65 – 70
70 – 75
75 – 80
> 80
Hold Values
Time (h) 3.0415
Temp. (K) 318

(c)

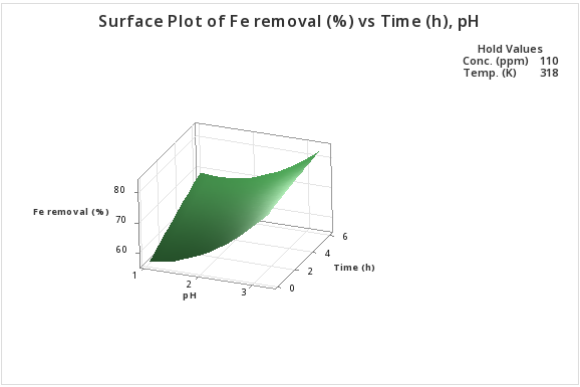
Surface Plot of Fe removal (%) vs Time (h), pH
Hold Values
Conc. (ppm) 110
Temp. (K) 318
Fe removal (%)
80
70
60
1
2
3
pH
6
4
2
0
Time (h)

(d)

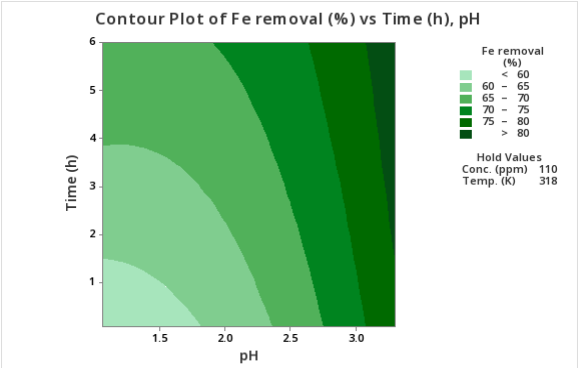
Contour Plot of Fe removal (%) vs Time (h), pH
Time (h)
6
5
4
3
2
1
1.5
2.0
2.5
3.0
pH
Fe removal (%)
< 60
60 – 65
65 – 70
70 – 75
75 – 80
> 80
Hold Values
Conc. (ppm) 110
Temp. (K) 318

(e)

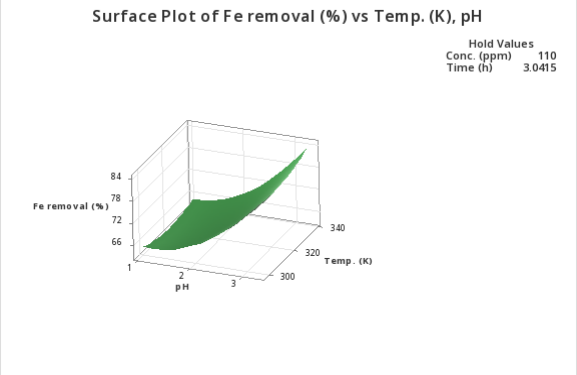
Surface Plot of Fe removal (%) vs Temp. (K), pH
Hold Values
Conc. (ppm) 110
Time (h) 3.0415
Fe removal (%)
84
78
72
66
1
2
3
pH
340
320
300
Temp. (K)

(f)

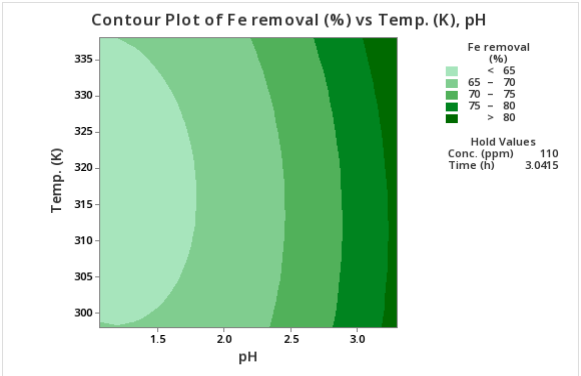
Contour Plot of Fe removal (%) vs Temp. (K), pH
Temp. (K)
335
330
325
320
315
310
305
300
1.5
2.0
2.5
3.0
pH
Fe removal (%)
< 65
65 – 70
70 – 75
75 – 80
> 80
Hold Values
Conc. (ppm) 110
Time (h) 3.0415

(g)

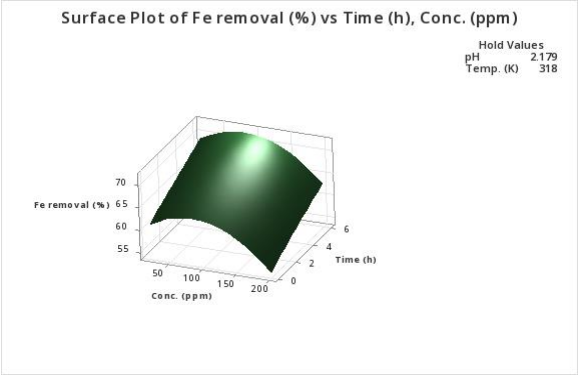
Surface Plot of Fe removal (%) vs Time (h), Conc. (ppm)
Hold Values
pH 2.179
Temp. (K) 318
Fe removal (%)
70
65
60
55
50
100
150
200
Conc. (ppm)
6
4
2
0
Time (h)

(h)

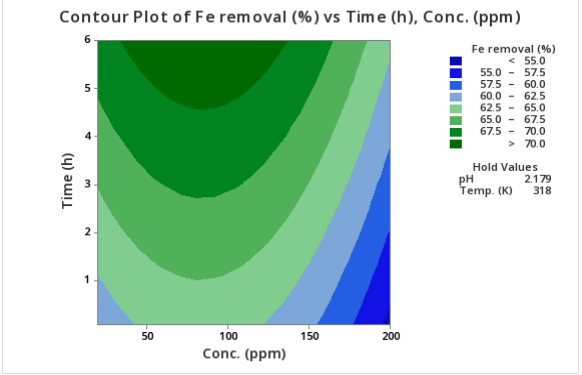
Contour Plot of Fe removal (%) vs Time (h), Conc. (ppm)
Time (h)
6
5
4
3
2
1
50
100
150
200
Conc. (ppm)
Fe removal (%)
< 55.0
55.0 – 57.5
57.5 – 60.0
60.0 – 62.5
62.5 – 65.0
65.0 – 67.5
67.5 – 70.0
> 70.0
Hold Values
pH 2.179
Temp. (K) 318

(i)

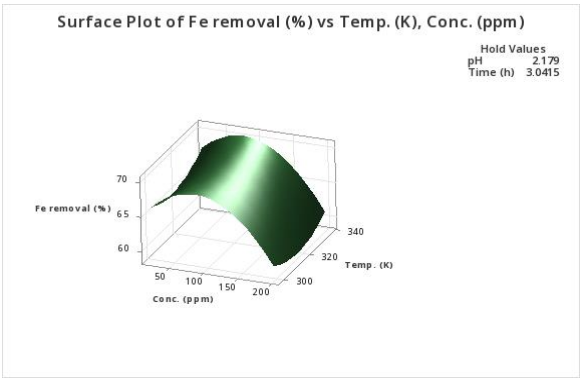

(j)

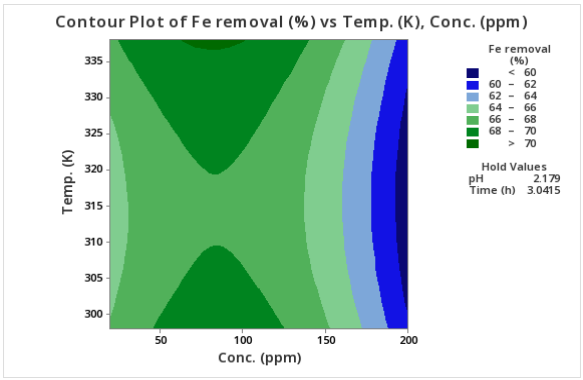

(k)

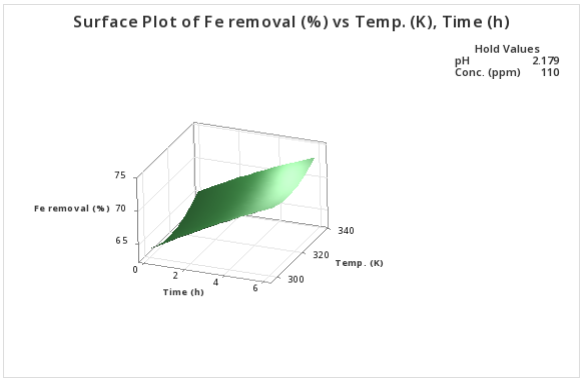

(l)

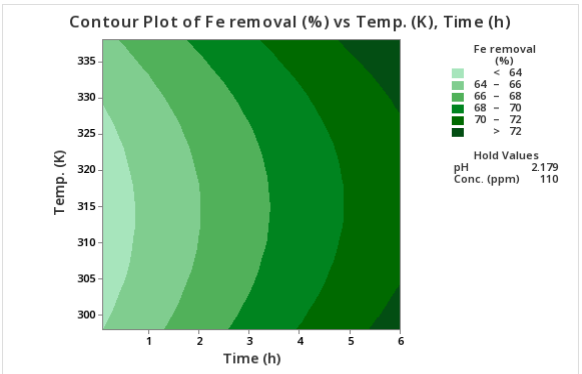

Fig. 8 (a–l). The response surface and contour plots for the removal of Fe^{2+} by using chitosan/jojoba oil/ZnO nanocomposite capsules.

(a)

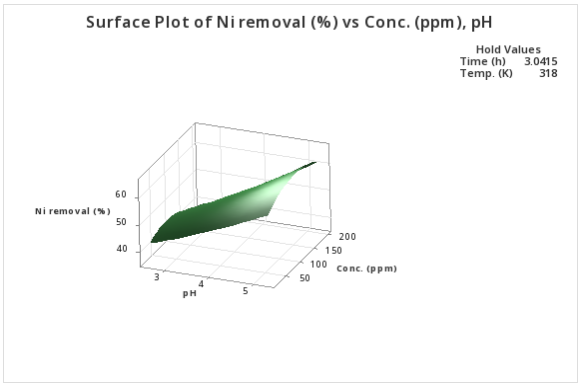

(b)

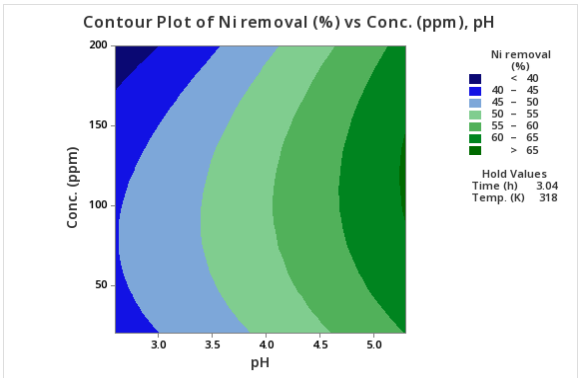

(c)

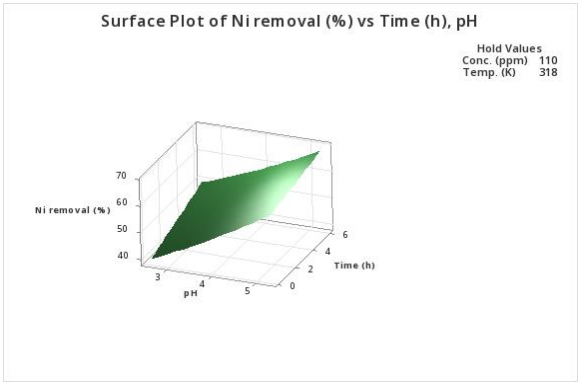

(d)

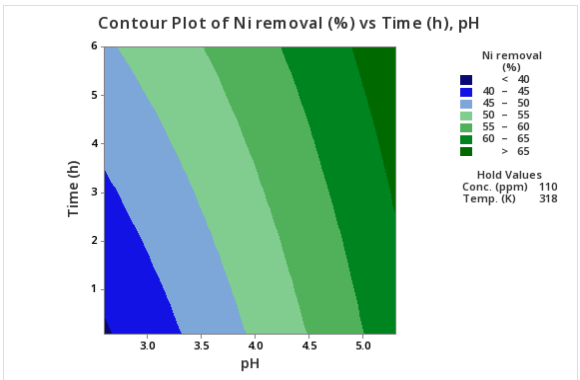

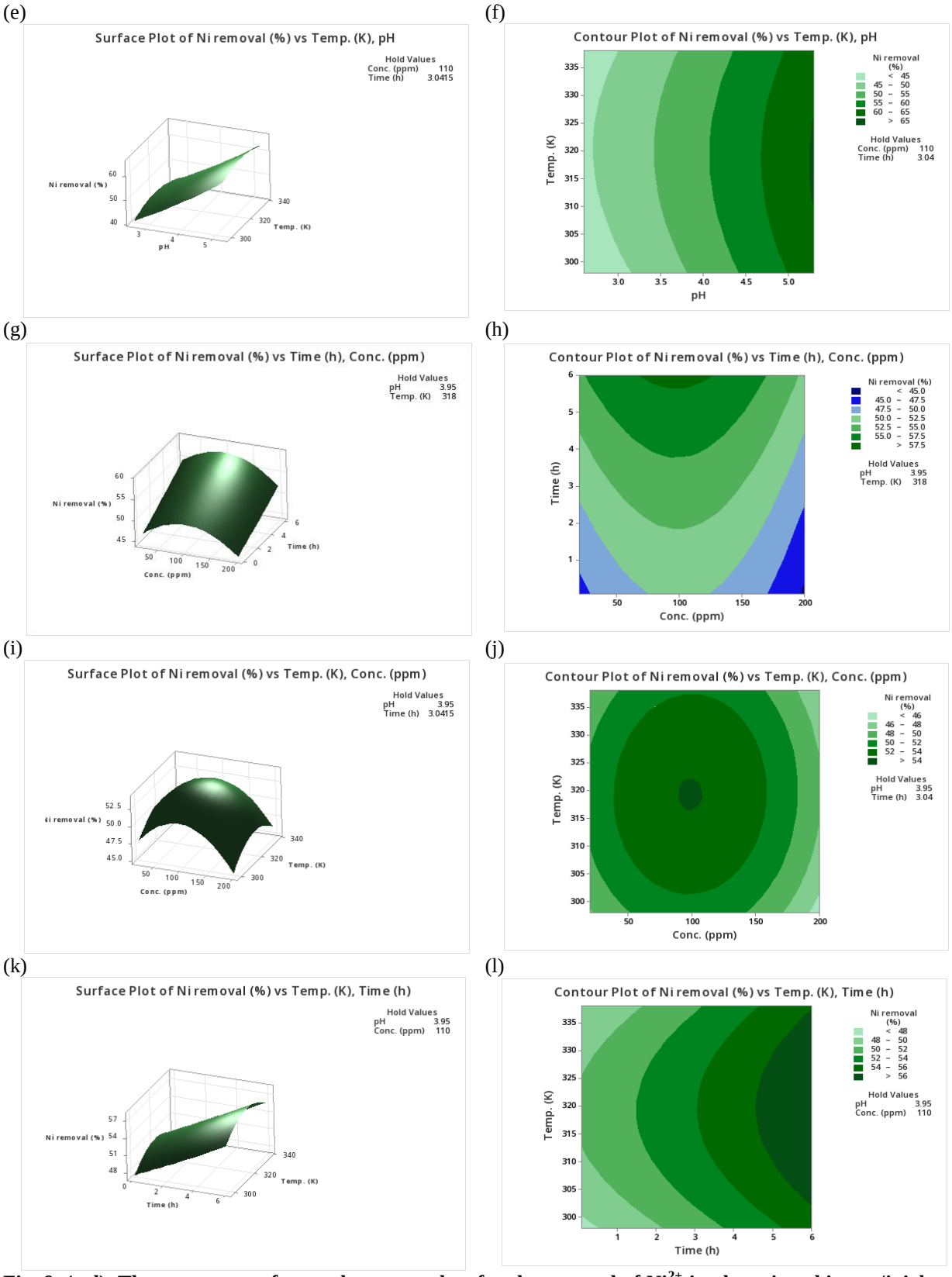

Fig. 9. (a–l). The response surface and contour plots for the removal of Ni^{2+} ion by using chitosan/jojoba oil/ZnO nanocomposite capsules.

3.8. Optimized responses

Table 8 lists the anticipated optimum conditions (pH, concentration, time, and temperature) for the removal of Fe^{2+} and Ni^{2+} ions, at which the maximum removal percentage by chitosan/jojoba oil and chitosan/jojoba oil/ZnO nanocomposite capsules attained its maximum value.

Table 8. The anticipated optimum conditions (pH, concentration, time, and temperature) for the removal of Fe^{2+} and Ni^{2+} ions.

Adsorbate	pH	Conc. (ppm)	Time (h)	Temp. (K)	Optimized responses (removal %)
removal % of Fe^{+2} by chitosan/jojoba oil	3.3	107.2	6	319.4	73.84
removal % of Fe^{+2} by chitosan/jojoba oil/ ZnO nanocomposite capsules	3.3	100.0	6	338	85.77
removal % of Ni^{+2} by chitosan/jojoba oil	5.3	61.81	6	324.6	43.57
removal % of Ni^{+2} by chitosan/jojoba oil/ ZnO nanocomposite capsules	5.3	116.3	6	318.6	68.30

Table 9. Effect of different amendments on EC and content of some elements in mallow plant.

Amendments / Rates	EC (dS/m)			Zn (ppm)		
	Chitosan 1	**Chitosan 2**	**Means (Rate)**	**Chitosan 1**	**Chitosan 2**	**Means (Rate)**
Control	1.96a	1.96a	1.96A	87.60d	87.60d	87.60C
1.0%	1.45b	1.31c	1.38C	65.80e	105.63c	85.71D
1.5%	1.36c	1.35c	1.35C	59.63f	129.27b	94.45B
2.0%	1.42b	1.44b	1.43B	51.74g	149.36a	100.55A
Means (A)	1.55A	1.51A		66.19B	117.97A	
Amendments / Rates	**fresh weight (g/pot)**			**dry weight (g/pot)**		
	Chitosan 1	**Chitosan 2**	**Means (Rate)**	**Chitosan 1**	**Chitosan 2**	**Means (Rate)**
Control	30.17e	30.17e	30.17C	17.73e	17.73e	17.73C
1.0%	22.75f	32.36d	27.55D	13.66f	17.94e	15.80D
1.5%	48.21a	41.66b	44.94A	38.46a	22.33c	30.39A
2.0%	32.11d	39.28c	35.69B	19.45d	23.59b	21.52B
Means (A)	33.31B	35.87A		22.32A	20.40A	
Amendments / Rates	**Fe (ppm)**			**Mn (ppm)**		
	Chitosan 1	**Chitosan 2**	**Means (Rate)**	**Chitosan 1**	**Chitosan 2**	**Means (Rate)**
Control	8879.1a	8879.1a	8879.1A	414.63a	414.63a	414.64A
1.0%	6148.6b	4374.2bc	5261.4B	399.87b	350.62c	375.24B
1.5%	3742.3c	3335.1c	3538.7C	337.73e	343.77d	340.75C
2.0%	1145.8d	4376.4bc	2761.1C	252.36f	218.15g	235.25D
Means (A)	5786.6A	4433.6A		351.15A	331.79B	
Amendments / Rates	**Co (ppm)**			**Cr (ppm)**		
	Chitosan 1	**Chitosan 2**	**Means (Rate)**	**Chitosan 1**	**Chitosan 2**	**Means (Rate)**
Control	20.58a	20.58a	20.58A	68.65a	68.65a	68.65A
1.0%	16.41b	13.98c	15.19B	59.14b	51.74d	55.44B
1.5%	13.98c	12.01d	12.99C	55.90c	42.77e	49.33C
2.0%	11.97e	9.98f	10.98D	44.15e	39.52f	41.84D
Means (A)	15.73A	14.14A		56.96A	50.67B	
Amendments / Rates	**Pb (ppm)**			**Ni (ppm)**		
	Chitosan 1	**Chitosan 2**	**Means (Rate)**	**Chitosan 1**	**Chitosan 2**	**Means (Rate)**
Control	65.60a	65.60a	65.60A	22.81a	22.81ab	22.81A
1.0%	65.92a	54.85c	60.38B	20.39ab	20.52ab	15.07B
1.5%	60.64b	28.65d	44.64C	20.52ab	7.24cd	13.88B
2.0%	55.78c	9.76e	32.77D	18.87b	4.68d	11.77C
Means (A)	61.98A	39.71B		20.65A	11.22B	

Chitosan 1= Chitosan/jojoba oil Chitosan 2= Chitosan/jojoba oil/ ZnO nanocomposite capsules

3.9. Effects of chitosan/jojoba oil and chitosan/jojoba oil/ZnO nanocomposite capsules on some soil properties and mallow productivity

The chitosan/jojoba oil/ZnO nanocomposite capsules offer significant environmental benefits. Chitosan has been used in agriculture as a fertilizer and controlled agrochemical release to boost plant production and encourage growth in normal and polluted situations.

Generally, after treatment with chitosan/jojoba oil and chitosan/jojoba oil/ZnO nanocomposite capsules, data presented in Table 9 show significant effects in some elements such as (Mn, Zn, Cr, Ni and Pb) in mallow plant.

The addition rates appeared significantly affect soil electrical conductivity (EC) and several elements (Fe, Mn, Zn, Co, Cr, Ni, and Pb) in the mallow plant. However, the contents of some elements (Fe and Co) in the mallow plant and the EC of the soil did not show significant effects with the treatments.

Moreover, the total concentration of Ni in the studied soil exceeded the critical level. Adding amendments, specifically chitosan/jojoba oil and chitosan/jojoba oil/ZnO nanocomposite capsules, showed a highly significant relationship with Ni contents in mallow plants.

4. Discussion

The results indicate that EL-Gabal EL- Asfer soils are polluted with heavy metals. Table 3, Theses values are more than the maximum permissible limits for total Fe^{2+} and Ni^{2+} in soil, adapted from Khalifa and Gad (2018), Ghorbani et al. (2002), and Naggar et al. (2014).

The FTIR spectrum of chitosan/jojoba oil reveals a prominent bandwidth at 3249.4 cm^{-1}, corresponding to the O-H groups' stretching vibration. Foroughi-dahr et al. (2016) ascribed the bands around 2937.4 cm^{-1} to CH groups' asymmetric and symmetric stretching vibration. At wavenumber intervals of 1715.2 cm^{-1}, a large cluster of functional groups such as -COO and -C=O was discovered. After copulating chitosan with ZnO NPs, the typical adsorption band of -CH around wave numbers 1036.3 cm^{-1} was shifted to 1099.1 cm^{-1}. The presence of oxygen functional groups, such as conjugated C-O stretching in carboxylic groups, has been attributed to the peak at 1737 cm^{-1} in chitosan/jojoba oil/ZnO nanocomposite capsules (Zhao et al., 2017). The peak at 1036 cm^{-1} is attributed to the aliphatic amine -CN stretch (Sharififard et al., 2013). When the FTIR spectra of chitosan/jojoba oil/ZnO nanocomposite capsules are interpreted, the spectrum shows the absorption of both chitosan and ZnO NPs. The stretching vibrations of -OH groups in the range 3600 to 3000 cm^{-1}, which are imbricate to the stretching vibrations of N-H and C-H bands in CH_2 (2923.7 cm^{-1}) and -CH_2 (2854 cm^{-1}) groups, respectively, caused the primary bands to appear in the spectrum (Auta and Hameed, 2013). The vibration of carbonyl bonds (C=O) in the amide group CONHR [secondary amide] and the vibration of the protonated amine group are responsible for the absorption band at 1461.6 cm^{-1}. The narrow peak at 528 cm^{-1} corresponds to chitosan saccharide structural oscillations (Paluszkiewicz et al., 2011). For ZnO nanoparticles, the stretching vibration due to Zn–O appeared at 468 (weak) and 490 (strong) cm^{-1} (Hong et al., 2009; Yadav et al., 2017).

Coating jojoba with chitosan (Fig. 3a) resulted in fewer porous wrinkles, indicating that the pores might have functioned as active sites in removing heavy metals (Attia et al., 2018). Additionally, the surface appeared faded (Leki et al., 2013). On the other hand, SEM images of chitosan/jojoba/ZnO nanocomposites, with the application of the glutaraldehyde as a crosslinking agent (Figure 3b), revealed the formation of microcapsules of chitosan-Zn nanocomposites (Persico et al., 2005). Bright white spherical ZnO nanoparticles are embedded in a rough chitosan matrix (El-Shishtawy, 2021).

The size and surface chemistry of ZnO NPs play critical roles in the removal of Fe^{2+} and Ni^{2+} ions from polluted soil. In the present study, the TEM image showed the physical aggregation of the chitosan/jojoba oil/ZnO nanocomposite capsules. There are two possible reasons for this behavior. First, the presence of ZnO nanoparticles in the pores of the chitosan/jojoba oil nanoparticles may be attributed to chitosan chain cross-linking, which generated magnetic nanoparticle aggregation. Second, the particle diameter was too tiny, and the surface energy was extremely high, potentially leading to physical aggregation. However, part of the observed aggregation might be due to drying during TEM sample preparation (Ghadi et al., 2014 and Elkhwaga et al., 2023).

The mechanism of complex formation between chitosan/jojoba oil/ZnO nanocomposite capsules and metal ions, Due to the presence of multiple functional groups, chitosan can be modified. It possesses reactive amino and hydroxyl groups, allowing chemical modifications to enhance its characteristics under moderate reaction conditions. Chitosan modification primarily aims to manage its hydrophobic, cationic, and anionic characteristics

and bind different functional groups and ligands (Nofal et al., 2024).

A cross-linker, such as glutaraldehyde, can increase the chemical stability of chitosan/jojoba oil during the preparation process (Ghadi et al., 2014), Equation 9.

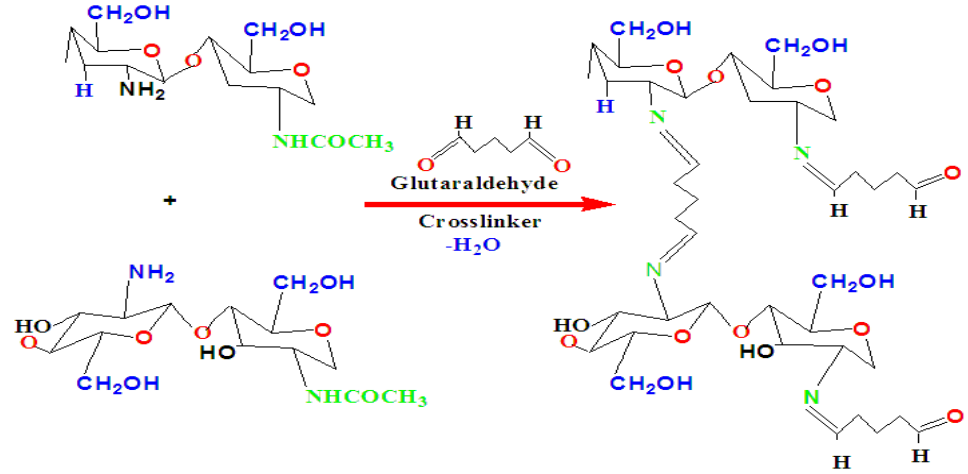

(9)

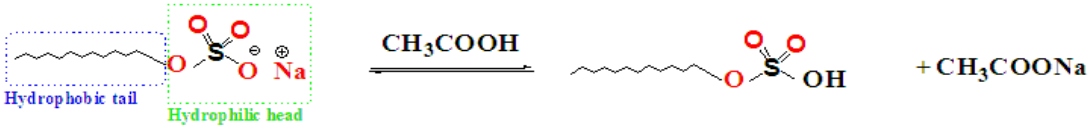

(10)

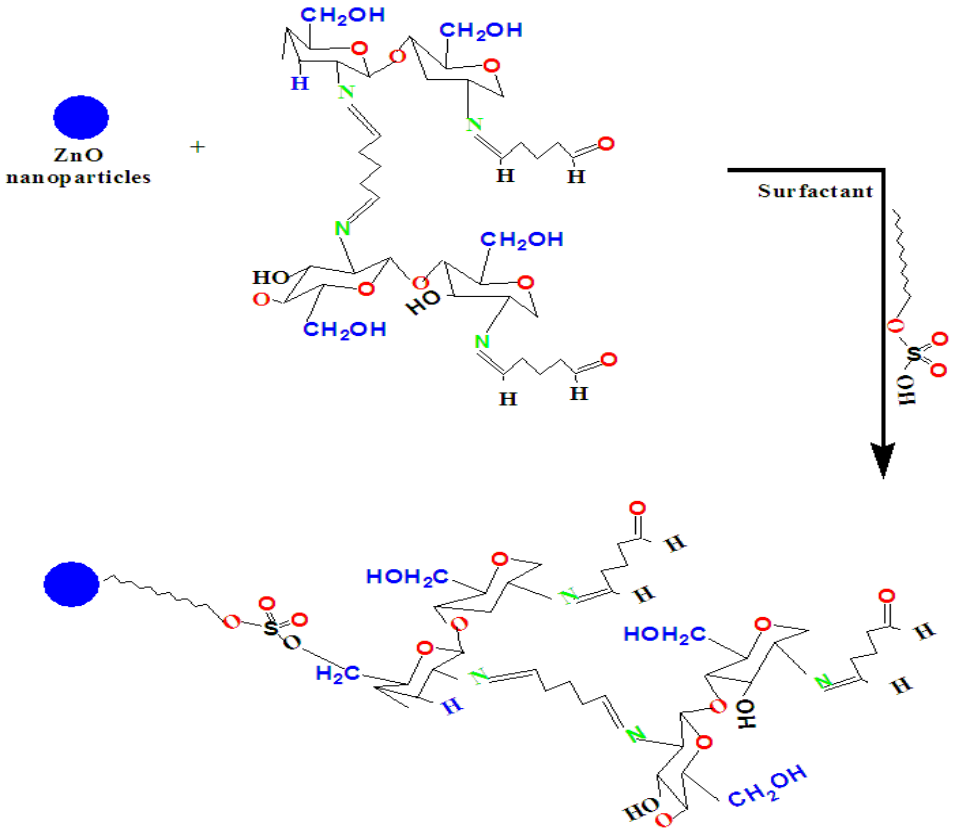

(11)

The resulting chitosan obtains a partial positive charge, allowing it to be easily dissolved in organic acids such as acetic acid. The interactions between the chitosan/jojoba oil and sodium dodecyl sulfate are ionic. The charge difference between chitosan/jojoba oil and sodium dodecyl sulfate

induces these interactions. Chitosan/jojoba oil is a cationic polymer, while sodium dodecyl sulfate is an anionic surfactant. Before reacting with chitosan/jojoba oil, sodium dodecyl sulfate will be protonated (in acetic acid), resulting in a loss of Na^{+}. Equation 10 shows that the protonated sodium dodecyl sulfate will bind to the O atom in the chitosan/jojoba oil molecule.

The complex formation between chitosan/jojoba oil and ZnO nanoparticles may be characterized using Lewis acid-base theory, which states that acids are electron acceptors and bases are electron donors. The nanocomposite capsules' surface contains −OH, $-NH_2$, and CH_3CO- groups, making it simple to adsorb heavy metal ions like Fe^{2+} and Ni^{2+} by surface complexation, electrostatic attraction, and ion exchange. In the chitosan/jojoba oil/ZnO nanocomposite capsules, metal ions are coordinated to one of the chitosan's amino or hydroxyl groups (Equation 11), Awan et al., 2021.

Additionally, the chitosan/jojoba oil/ZnO nanocomposite capsules' porous structure and pore distribution from SEM images indicate that the material has many adsorption sites, making it an excellent choice for usage in the purification of water that has been contaminated with Fe^{2+} and Ni^{2+}. While investigating the impact of the initial Fe^{2+} concentration, it was observed that the Fe^{2+} removal percentage decreased as the Fe^{2+} concentration increased for both chitosan/jojoba oil and chitosan/jojoba oil/ZnO nanocomposite capsules absorbents. This decrease in removal percentage can be attributed to more ions occupying the surface, resulting in a minor decrease in the elimination of Fe^{2+}, Table 4.

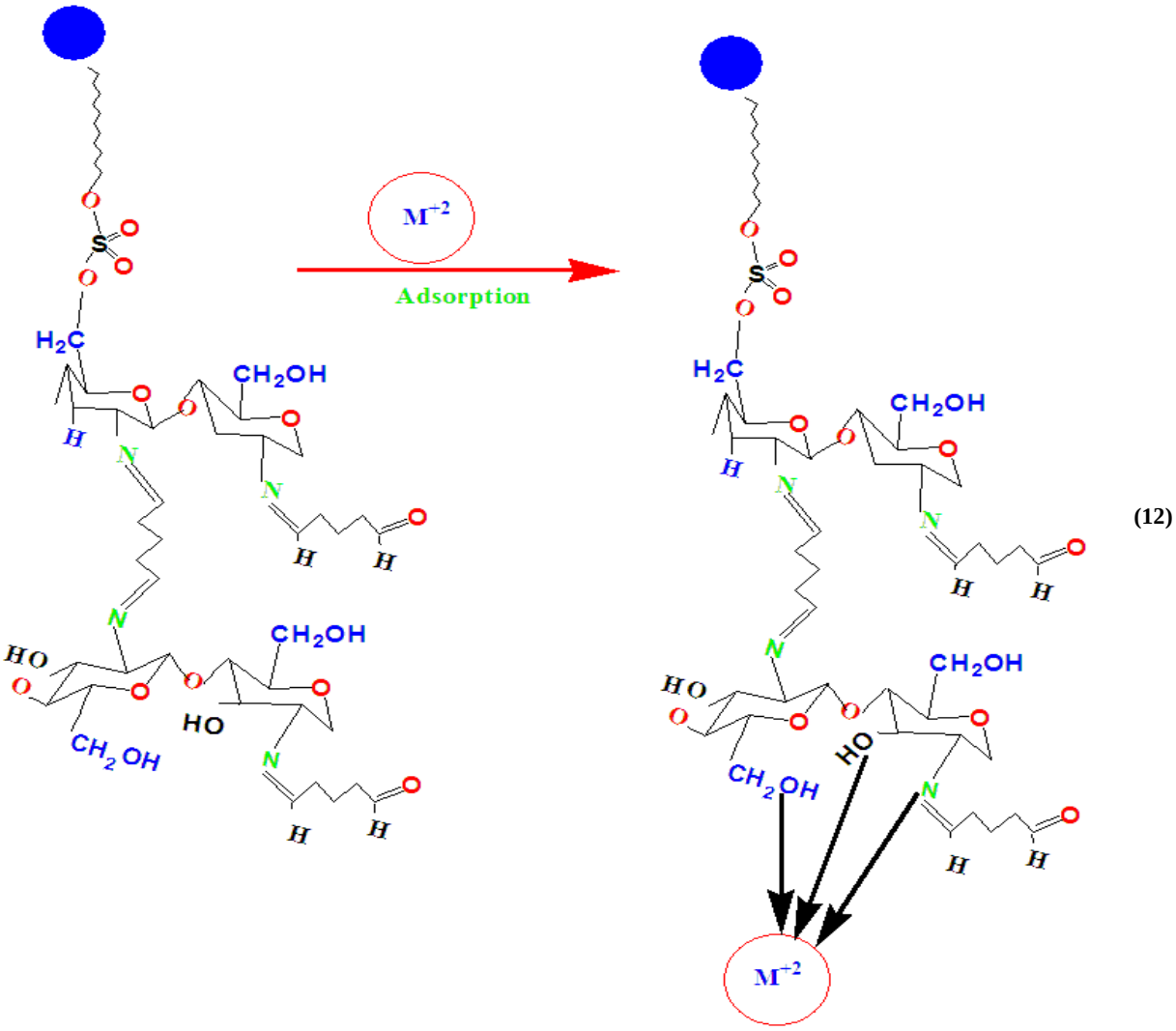

(12)

Figure 5, The rate of Fe^{2+} removal increases when the pH of the salt solution is higher than pH 3.3. This is attributed to the negatively charged surface functional groups on adsorbents and electrostatic interactions between positively charged ions. This

observation is consistent with the findings of Eissa et al., 2022.

Equation 12 shows that the adsorption capacity of chitosan/jojoba oil and chitosan/jojoba oil/ZnO nanocomposite capsules for M^{2+} (Fe^{2+} or Ni^{2+}) increased when the initial pH of the solution began to rise. This is attributed to the increase in the pH of the initial solution. As the pH rises, the functional groups on the chitosan/jojoba oil and chitosan/jojoba oil/ZnO nanocomposite capsules surface, particularly the carboxyl, amine, and hydroxyl groups, became deprotonated. This results in the development of a negatively charged surface, making it capable of binding positively charged metal ions from the aqueous solution. The highest removal percentage of Fe (II) and Ni (II) occurs at pH 3.3 and 5.3, respectively.

Quantitative precipitation occurred at pH levels greater than 3.3 and 5.3 for Fe(II) and Ni(II), respectively. The chitosan/jojoba oil and chitosan/jojoba oil/ZnO nanocomposite capsules served as precipitation centers for Fe(II) and Ni(II) ions. Sufficient hydroxyl and carboxyl groups on the adsorbent's surface facilitated the transformation into a sparingly soluble compound. In a very low acidic media, the amino groups of chitosan become protonated (NH_3^+), leading to a decrease in removal capacity (Vakili et al., 2019).

The computed *F* ratio and *p*-value of any factor's effect can be used to determine its significance. According to Igartua and Hayes (2021) and Eissa (2024), a large *F* ratio implies that the regression equations shown in Table 7 can be used to characterize the variability in response. The accompanying *p*-value determines whether the *F* ratio is large enough to suggest any significant effect. The effects with a 95% confidence level *p*-value less than 0.05 are considered significant, in agreement with Chicco et al., 2021.

Table 5, This pattern indicates that the experimental errors varied continuously with the mean response. The plots' random distribution pattern proved that the regression model was appropriate (Ali et al., 2023).

Figure 7, The standardized chart displays standardized effects distributed through their standard error (Lanjwani et al., 2023). The chart includes a reference line indicating the significance level, with effects exceeding the line considered significant (Ali et al., 2023; Lanjwani et al., 2023).

The toxicity of NPs, particularly at higher doses, may significantly challenge their usage as nanofertilizers (Avila-Quezada et al., 2022). According to Thounaojam et al. (2021), greater concentrations of ZnO NPs (> 500 mg/kg) are hazardous to plants, but lower concentrations are advantageous, depending on the plant type and growing conditions. Thus, modest quantities of NPs may be used with other treatments to reduce Fe and Ni accumulation in crops. Zn NPs were expected to increase Zn concentrations in plants, whereas chitosan/jojoba oil would immobilize Fe and Ni in the soil.

Table 9 shows the significant effects of adding chitosan/jojoba oil/ZnO nanocomposite capsules and Zn content in the mallow plant. This is attributed to the ability of chitosan/jojoba oil/ZnO nanocomposite capsules to control the release of Zn^{2+} ions into the soil solution environment during the growth of mallow plants. That agrees with Malekpoor et al., 2016; Sári et al., 2024b and Yang et al., 2021.

5. Conclusions

The study evaluated the effectiveness of different chitosan/jojoba oil and chitosan/jojoba oil/ZnO nanocomposite capsule adsorbents in removing Fe^{2+} and Ni^{2+} ions from solutions. The adsorbents' structure was characterized using SEM, FTIR, particle size and TEM. The study investigated specific parameters (pH, concentration, time, and temperature) to determine the conditions under which chitosan/jojoba oil/ZnO nanocomposite capsules achieved their maximum removal percentages for Fe^{2+} and Ni^{2+} ions. The maximum removal percentages were 85.77% for Fe^{2+} ions and 68.30% for Ni^{2+} ions under the identified optimal conditions. The Freundlich isotherm model could provide a valuable interpretation of the adsorption data. Fe and Ni uptake by mallow plant (*Corchorus olitorius*) was dramatically reduced when the adsorbents of chitosan/jojoba oil/ZnO nanocomposite capsules were administered at a rate of 2.0% with increasing Zn uptake.

In conclusion, chitosan/jojoba oil derived from leftover agricultural materials successfully enhanced the ability of the mallow plant to grow in polluted soils. The ability of chitosan/jojoba oil/ZnO nanocomposite capsules to take up ions from soil solutions was discussed in the presence of a mallow plant. Moreover, chitosan/jojoba oil and chitosan/jojoba oil/ZnO nanocomposite capsule amendments were beneficial as growing media because they improved soil fertility and provided plant nutrients like Zn. Chitosan/jojoba oil/ZnO nanocomposite capsules is a promising technique for heavy metal reclamation.

6. Conflicts of interest

There are no conflicts to declare.

7. Formatting of funding sources

There is no funding agency.

8. References

Ahmed, Z. and Sarkar, S. (2022). Review on jute leaf: A powerful biological tool. International Journal of Scientific Research Updates, 4(1), 64-85.

Akhtar, N., Syakir Ishak, M. I., Bhawani, S. A. and Umar, K. (2021). Various natural and anthropogenic factors responsible for water quality degradation: A review. Water, 13(19), 2660.

Alengebawy, A., Abdelkhalek, S. T., Qureshi, S. R. and Wang, M. Q. (2021). Heavy metals and pesticides toxicity in agricultural soil and plants: Ecological risks and human health implications. Toxics, 9(3), 42.

Ali, A. E., Chowdhury, Z. Z., Rafique, R. F., Ikram, R., Faisal, A. N. M., Shibly, S., Barua, A., Wahab, Y. A. and Jan, B. M. (2022). Science and technology roadmap for adsorption of metallic contaminants from aqueous effluents using biopolymers and its' derivatives. Advanced Industrial Wastewater Treatment and Reclamation of Water: Comparative Study of Water Pollution Index during Pre-industrial, Industrial Period and Prospect of Wastewater Treatment for Water Resource Conservation, 165-196.

Ali, F., Khan, N., Khan, A. M., Ali, K. and Abbas, F. (2023). Species distribution modelling of Monotheca buxifolia (Falc.) A. DC.: Present distribution and impacts of potential climate change. Heliyon, 9(2).

Ashour, M., Mansour, A. T., Abdelwahab, A. M. and Alprol, A. E. (2023). Metal Oxide Nanoparticles' Green Synthesis by Plants: Prospects in Phyto-and Bioremediation and Photocatalytic Degradation of Organic Pollutants. Processes, 11(12), 3356.

Attia, Abdel Meguid, A., Shouman, M. A.,. Khedr, S. A. and Hassan, N. A. (2018) "Fixed-bed column studies for the removal of Congo red using Simmondsia chinesis (Jojoba) and coated with Chitosan." Indonesian Journal of Chemistry 18(2): 294-305.

Auta, M. and Hameed, B.H. (2013). Coalesced chitosan activated carbon composite for batch and fixed-bed adsorption of cationic and anionic dyes, Colloids Surf., B, 105, 199–206.

Avila-Quezada, G. D., Ingle, A. P., Golińska, P. and Rai, M. (2022). Strategic applications of nano-fertilizers for sustainable agriculture: Benefits and bottlenecks. Nanotechnology Reviews, 11(1), 2123-2140.

Awan, S., Shahzadi, K., Javad, S., Tariq, A., Ahmad, A. and Ilyas, S. (2021). A preliminary study of influence of zinc oxide nanoparticles on growth parameters of *Brassica oleracea* var italic. Journal of the Saudi Society of Agricultural Sciences, 20(1), 18-24.

Buasri, A., Unkaew, C., Sawatkoed, P., Pipattananchaiyanan, P. and Loryuenyong, V. (2024). Application of response surface methodology for optimization of biodiesel production parameters from waste vegetable oil using N-(2-hydroxy) propyl-3-trimethyl ammonium chitosan chloride-based catalyst. South African Journal of Chemical Engineering, 47, 50-59.

Chicco, D., Warrens, M. J., & Jurman, G. (2021). The coefficient of determination R-squared is more informative than SMAPE, MAE, MAPE, MSE and RMSE in regression analysis evaluation. PeerJ Computer Science, 7, e623.

Cottenie, A., Verloo, M., Kiekens, L., Velghe, G. and Camerlynck, R. (1982). Chemical Analysis of Plants and Soils (Lab. Agroch. State Univ., 1982).

Eissa, D. T. (2024). Effect of calcium silicate nanoparticles applications on salt affected soils environmental conditions. Egyptian Journal of Soil Science, 64(1), 335-354.

Eissa, D., Hegab, R. H., Abou-Shady, A. and Kotp, Y. H. (2022). Green synthesis of ZnO, MgO and SiO_2 nanoparticles and its effect on irrigation water, soil properties, and Origanum majorana productivity. Scientific Reports, 12(1), 5780.

Elkhwaga, A. A., Eldakar, H. A., Alkollaly, A. M., Draz, I. S., & Adbelghany, R. E. (2023). Nanochitosan and Water-Soluble Vitamins Induce Resistance to Leaf Rust and Related Metabolism in Wheat. Egyptian Journal of Phytopathology, 51(1), 65-75.

El-Shishtawy, R. M., Ahmed, N. S. and Almulaiky, Y. Q. (2021). Immobilization of catalase on chitosan/ZnO and chitosan/ZnO/Fe_2O_3 nanocomposites: a comparative study. Catalysts, 11(7), 820.

Faizan, M., Alam, P., Rajput, V. D., Tonny, S. H., Yusuf, M., Sehar, S., Adil, M.F. and Hayat, S. (2023). Nanoparticles: An Emerging Soil Crops Saviour under Drought and Heavy Metal Stresses. Egyptian Journal of Soil Science.

Farooq, M. A., Hannan, F., Islam, F., Ayyaz, A., Zhang, N., Chen, W., Zhang, K., Huang, Q., Xuc, L. and Zhou, W. (2022). The potential of nanomaterials for sustainable modern agriculture: present findings and future perspectives. Environmental Science: Nano, 9(6), 1926-1951.

Foroughi-dahr, M., Esmaieli, M., Abolghasemi, H., Shojamoradi, A. and Pouya, E.S. (2016). Continuous adsorption study of Congo red using tea waste in a fixed-bed column, Desalin. Water Treat., 57 (18), 8437–8446.

Ghadhban, M. Y., Rashid, K. T., A. AbdulRazak, A. and Alsalhy, Q. F. (2023). Recent progress and future

directions of membranes green polymers for oily wastewater treatment. Water Science & Technology, 87(1), 57-82.

Ghadi, A., Mahjoub, S., Tabandeh, F. and Talebnia, F. (2014). Synthesis and optimization of chitosan nanoparticles: Potential applications in nanomedicine and biomedical engineering. Caspian journal of internal medicine, 5(3), 156.

Ghorbani, N.R., N. Salehrastin and A. Moeini (2002). Heavy metals affect the microbial populations and their activities. Symposium N 54 at 17th World Congress of Soil Science, Thailand, 2234: 1-11.

Hamdy, N. M., El Sayed, E. Z., Allm, S. A., Bashir, M. M., Taha, H. E., Khater, R. M., El Sayed, W. M., El-gneady, F. F., El-tantawy, H. M., Awed, S. M. S. and Ismail, A. (2023). Nanotechnology and its prospective role in using bioactive compounds to fight covid 19 infection in this era. Egyptian Journal of Desert Research, 73(2), 513-549.

Hong, R.Y., Li, J.H., Chen, L.L., Liu, D.Q., Li, H.Z., Zheng, Y. and Ding, J.J. (2009). Synthesis, surface modification and photocatalytic property of ZnO nanoparticles.Powder Technol., 189, 426–432.

Hyder, S., Ul-Nisa, M., Shahid, H., Gohar, F., Gondal, A. S., Riaz, N., Younas, A., Santos-Villalobos, S., Montoya-Martínez, A., Sehar, A., Latif, F., Rizvi, Z. F. and Iqbal, R. (2023). Recent trends and perspectives in the application of metal and metal oxide nanomaterials for sustainable agriculture. Plant Physiology and Biochemistry, 107960.

Igartua, J. J., & Hayes, A. F. (2021). Mediation, moderation, and conditional process analysis: Concepts, computations, and some common confusions. The Spanish Journal of Psychology, 24, e49.

Khalifa, M. and Gad, A. (2018). Assessment of heavy metals contamination in agricultural soil of southwestern Nile Delta, Egypt. Soil and Sediment Contamination: An International Journal, 27(7), 619-642.

Khandegar, V., Kaur, P. J. and Chanana, P. (2021). Chitosan and graphene oxide-based nanocomposites for water purification and medical applications: a review. BioResources, 16(4), 8525.

Kurhade, P., Kodape, S. and Choudhury, R. (2021). Overview on green synthesis of metallic nanoparticles. Chemical Papers, 75(10), 5187-5222.

Lanjwani, M. F., Khuhawar, M. Y., Khuhawar, T. M. J., Lanjwani, A. H., Memon, S. Q., Soomro, W. A., & Rind, I. K. (2023). Photocatalytic degradation of eriochrome black T dye by ZnO nanoparticles using multivariate factorial, kinetics and isotherm models. Journal of Cluster Science, 34(2), 1121-1132.

Maftouh, A., El Fatni, O., El Hajjaji, S., Jawish, M. W. and Sillanpää, M. (2023). Comparative review of different adsorption techniques used in heavy metals removal in water. Biointerface Res. Appl. Chem, 13, 397.

Mahmoud, S., Shedeed, S., El-Ramady, H., Abdalla, Z. F., El-Bassiony, A. E. M. and El-Sawy, S. (2023). Biological Nano-selenium for eggplant biofortification under soil nutrient deficiency. Egyptian Journal of Soil Science, 63(2), 151-162.

Malekpoor, F., Pirbalouti, A. G. and Salimi, A. (2016). Effect of foliar application of chitosan on morphological and physiological characteristics of basil under reduced irrigation. Research on Crops, 17(2), 354-359.

Marturano, V., Marotta, A., Salazar, S. A., Ambrogi, V. and Cerruti, P. (2023). Recent advances in bio-based functional additives for polymers. Progress in Materials Science, 101186.

Naggar, Y. A., Naiem, E., Mona, M., Giesy, J. P., & Seif, A. (2014). Metals in agricultural soils and plants in Egypt. Toxicological & Environmental Chemistry, 96(5), 730-742.

Nirmala, E., Dhivya, S., Sarojini, S. and Duraivel, S. (2021). A Review On Sodium Lauryl Sulphate-A Surfactant. World Journal of Pharmaceutical Research, 10(13), 506-512.

Nnaji, N. D., Onyeaka, H., Miri, T. and Ugwa, C. (2023). Bioaccumulation for heavy metal removal: a review. SN Applied Sciences, 5(5), 125.

Nofal, E., Menesy, F., Elbably, S., Rahman, A. E., El-Ramady, H., & Prokisch, J. (2024). Response of *Kigelia africana* (Lam.) Benth Transplants to Nano-NPK and Nano-Chitosan under Salinity Stress. Egyptian Journal of Soil Science, 64(2), 661 – 672.

Paluszkiewicz, C., Stodolak, E., Hasik, M. and Blazewicz, M. (2011). FT-IR study of montmorillonite-chitosan nanocomposite materials, Spectrochim. Acta, Part A, 79(4), 784–788.

Persico, P., Carfagna, C., Danicher, L. and Frere., Y. (2005). Polyamide microcapsules containing jojoba oil prepared by inter-facial polymerization. Journal of microencapsulation, 22 (5): 471-486.

Rahman, M. S., Alom, J., Nitai, A. S., Hasan, M. S., Ahmed, M. B., Nam, S. and Mondal, M. I. H. (2022). Ultraviolet-blocking protective textiles. In Protective Textiles from Natural Resources (pp. 395-444). Woodhead Publishing.

Sári, D., Ferroudj, A., Dávid, S., El-Ramady, H., Abowaly, M., Abdalla, Z. F., Mansour, H., Eid, Y. and Prokisch, J. (2024b). Is Nano-Management a Sustainable Solution for Mitigation of Climate Change under the Water-Energy-Food Nexus?. Egyptian Journal of Soil Science, 64(1)., 1-17.

Sári, D., Ferroudj, A., Dávid, S., El-Ramady, H., Faizy, S. E. D., Ibrahim, S., Mansour, H., Brevik, E. C., Solberg, S. Ø. and Prokisch, J. (2024a). Drought Stress Under a Nano-Farming Approach: A Review. Egyptian Journal of Soil Science, 64(1) 135-151.

Sharififard, H., Ashtiani, F.Z. and Soleimani, M. (2013). Adsorption of palladium and platinum from aqueous solutions by chitosan and activated carbon coated with chitosan, Asia-Pac. J. Chem. Eng., 8 (3), 384–395.

Soltanpour, P. N. (1985). Use of AB-DTPA soil test to evaluate element availability and toxicity. Commun. Soil Sci. Plant Anal. 16, 323–338.

Staff, S. S. (2014). Kellogg soil survey laboratory methods manual. Soil Surv. Investig. Rep. 42, 5.

Thounaojam, T. C., Meetei, T. T., Devi, Y. B., Panda, S. K., & Upadhyaya, H. (2021). Zinc oxide nanoparticles (ZnO-NPs): a promising nanoparticle in renovating plant science. Acta Physiologiae Plantarum, 43, 1-21.

Vakili, M., Deng, S., Cagnetta, G., Wang, W., Meng, P., Liu, D. and Yu, G. (2019). Regeneration of chitosan-based adsorbents used in heavy metal adsorption: A review. Separation and Purification Technology, 224, 373-387.

Wenning, L., Ejsing, C. S., David, F., Sprenger, R. R., Nielsen, J. and Siewers, V. (2019). Increasing jojoba-like wax ester production in Saccharomyces cerevisiae by enhancing very long-chain, monounsaturated fatty acid synthesis. Microbial Cell Factories, 18(1), 1-17.

Wojcieszek, J., Chay, S., Jiménez-Lamana, J., Curie, C. and Mari, S. (2023). Study of the Stability, Uptake and Transformations of Zero Valent Iron Nanoparticles in a Model Plant by Means of an Optimised Single Particle ICP-MS/MS Method. Nanomaterials, 13(11), 1736.

Xu, D.-M., Fu, R.-B., Liu, H.-Q. and Guo, X.-P. (2020). Current knowledge from heavy metal pollution in Chinese smelter contaminated soils, health risk implications and associated remediation progress in recent decades: a critical review. Journal of Cleaner Production, 124989. doi:10.1016/j.jclepro.2020.124989.

Yadav, M., Singh, V. and Sharma, Y.C. (2017). Methyl transesterification of waste cooking oil using a laboratory synthesized reusable heterogeneous base catalyst: Process optimization and homogeneity study of catalyst. Energy Convers. Manag., 148, 1438–1452.

Yang, G., Yuan, H., Ji, H., Liu, H., Zhang, Y., Wang, G., Chen, L. and Guo, Z. (2021). Effect of ZnO nanoparticles on the productivity, Zn biofortification, and nutritional quality of rice in a life cycle study. Plant Physiology and Biochemistry, 163, 87-94.

Zain, M., Ma, H., Rahman, S., Nuruzzaman, M., Chaudhary, S., Nuruzaman, M., Azeem, I., Mehmood, F., Duan, A. and Sun, C. (2023). Nanotechnology in precision agriculture: Advancing towards sustainable crop production. Plant Physiology and Biochemistry, 108244.

Zhao, B., Xiao, W., Shang, Y., Zhu, H. and Han, R. (2017). Adsorption of light green anionic dye using cationic surfactant-modified peanut husk in batch mode, Arabian J. Chem., 10 (Suppl. 2), 3595–3602.

Zungu, B., Paumo, H. K., Gaorongwe, J. L., Tsuene, G. N., Ruzvidzo, O. and Katata-Seru, L. (2023). Zn nutrients-loaded chitosan nanocomposites and their efficacy as nanopriming agents for maize (*Zea mays*) seeds. Frontiers in Chemistry, 11.